Available online at www.sciencedirect.com
ScienceDirect
Earth and Planetary Science Letters 248 (2006) 661–684
EPSL
www.elsevier.com/locate/epsl

Submarine earthquake geology along the North Anatolia Fault in the Marmara Sea, Turkey: A model for transform basin sedimentation

Cecilia M.G. McHugh [a,b,*], Leonardo Seeber [b], Marie-Helene Cormier [b], Jessica Dutton [a], Namik Cagatay [c], Alina Polonia [d], William B.F. Ryan [b], Naci Gorur [e]

[a] *Queens College, C.U.N.Y., 65-30 Kissena Blvd., Flushing, NY 11367, USA*
[b] *Lamont-Doherty Earth Observatory of Columbia University, Palisades, NY 10964, USA*
[c] *Istanbul Technical University, Ayazaga, Istanbul 80626, Turkey*
[d] *Institute of Marine Sciences, CNR, via Gobetti 101, Bologna 40129, Italy*
[e] *General Directorate of Mineral Research and Exploration, Ankara 06520, Turkey*

Received 19 July 2005; received in revised form 18 April 2006; accepted 11 May 2006
Available online 28 July 2006
Editor: V. Courtillot

Abstract

The submerged portions of the North Anatolia Fault system beneath the Marmara Sea were studied with high-resolution multibeam bathymetry, subbottom profiling and sediment cores. The major objectives were to learn about the seismic and tectonic history of the fault from the stratigraphic record at a scale similar to paleoseismic studies on land and to develop tools for submarine earthquake geology that can be applied to fault-controlled basins in general. We focused on Holocene sediment in several Marmara Sea basins of different sizes. The approach was to test whether: (1) the depocenters of the larger basins contain a record of all historic Ms>7 earthquakes within the Marmara Sea region; (2) the small transform basins record earthquakes that rupture through them; (3) vertical and strike-slip Holocene deformation can be quantified; and (4) the effects of an earthquake generally includes both primary structural features due to rupture of the sea floor, such as strata offset, scarps and tilting, as well as secondary effects due to shaking, such as mass-wasting and gravitational flows. We found evidence of earthquakes that we correlate with historic events in 181 AD, 740 AD, 1063 AD, 1343 AD, 1509 AD, 1766 AD, 1894 AD and 1912 AD. The geologic evidence is primarily from those basins adjacent to the rupture as inferred from historic data. This suggests that coseismic deformation of the sea floor along the rupture is a critical factor in the sedimentary record. We propose a qualitative sedimentation model that relates this coseismic deformation to mass-wasting of the slope, scour of the basin floor, seiche motions and homogenite deposition. Frequent earthquake activity sheds sediments from the flanks, contributes to the much thicker sediment on the basin floor and decreases the likelihood of sediment failures in response to normal marine gravity-driven processes. The surveying techniques and approaches used have therefore the potential of documenting earthquake ruptures of fault segments and to extend the earthquake record far before the known history, thus improving hazard evaluations and the fundamental understanding of earthquake process.

Keywords: North Anatolia Fault; Marmara Sea; earthquakes; paleoseismology; homogenite; Holocene sediments; seismic gap

* Corresponding author. Queens College, C.U.N.Y., 65-30 Kissena Blvd., Flushing, NY 11367, USA. Tel.: +1 718 997 3322; fax: +1 718 997 3299.
E-mail addresses: cmchugh@qc.cuny.edu, cecilia@ldeo.columbia.edu (C.M.G. McHugh).

0012-821X/$ - see front matter © 2006 Elsevier B.V. All rights reserved.
doi:10.1016/j.epsl.2006.05.038

1. Introduction

1.1. Submerged continental transform boundaries

Continental transform boundaries are regions of high seismic risk [1–11]. They are associated with broad zones of deformation that commonly cross heavily populated areas and cause destructive earthquakes. Examples include the southern California borderland associated to the San Andreas Fault system, the Venezuela borderland and Cariaco Basin associated to the El Pilar fault system, and the Marmara and North Aegean Seas associated with the North Anatolia Fault. As a result, continental transforms are extensively investigated, even though they contribute very little of the global moment release. Recent advances in high-resolution submarine imaging and sampling techniques provide opportunities to study the submerged portions of continental transforms with their complex systems of faults, basins, and ridges. The deformation and earthquake record over the entire transform basin history is uniquely preserved in syntectonic sediment. Studying this record can provide fundamental understanding of fault segmentation and earthquake recurrence and contribute to improve hazard estimates.

Paleoseismic methodologies are well established for land and lakes, but they are at the pioneering stage for the submarine environment [12–16]. The goals of this study are to unravel the Holocene seismic and tectonic history of the submerged portions of the North Anatolia Fault system in the Marmara Sea from its stratigraphic record at a scale equivalent to paleoseismic studies on land, and to develop tools and approaches for submarine earthquake geology that can be applied to other tectonic basins. As part of this effort, we conducted two high-resolution multibeam bathymetry, subbottom profiling and gravity coring surveys of the NAF beneath the Marmara Sea [12,17,18]. The goals were: (1) to characterize earthquake ruptures in space and time by looking at the stratigraphic record of fault-related basins, large, intermediate and small; (2) to establish reliable chronologies to date earthquake-related features; and (3) to quantify Holocene deformation and slip rates using datable markers such as shorelines and turbidites, and piercing points, such as offset channels and slumps. Precisely targeted core samples were interpreted within the framework of high-resolution geophysical images. The long and reliable historic record of the Marmara Sea region provides excellent opportunities for ground-truthing [19–23].

1.2. The North Anatolia Fault

The North Anatolia Fault (NAF) is a right lateral transform boundary that extends east–west across northern Turkey for nearly 1600 km [7,24–32] (Fig. 1). The NAF accommodates westward and counter clockwise motion of the Anatolia block relative to the Eurasian plate. The current motion in the Marmara region is 24 mm/yr [35–37], the accumulated right lateral displacement is in the range 50 to 85 km [26], and the commonly quoted age of the NAF is 10–13 my [35–38,27,28]. This implies either a recent increase in slip rate or a younger age for the NAF. In northwestern Turkey, the NAF branches westward into two main strands, through the northern and southern Marmara Sea, respectively [27,28,31–39]. The northern branch is submerged for 175 km along the length of the Marmara Sea, from the Gulf of Izmit in the east to the Ganos Mt. on the west. GPS measurements indicate that approximately 80% of the current relative plate motion is accommodated by the northern branch [37,38]. Geological reconstructions for the northern branch, however, suggest average long-term rates smaller than GPS rates, which may be accounted for by changes in strain partitioning between the northern and southern branches [26,12]. Different tectonic interpretations have been proposed for the NAF beneath the Marmara Sea. Some models propose pure strike-slip on a single recently formed through going fault (i.e., [30,31]). Other models interpret the Marmara Sea as a series of pull-apart basins with significant ongoing subsidence and fault segments combining normal and right-lateral motion [27–29,34,18].

The northern segment of the North Anatolia Fault has ruptured to the east and west of the Marmara Sea (Fig. 1). The most recent devastating earthquakes, the Mw 7.4 Izmit and the Mw 7.2 Duzce events in 1999, ruptured on land east of the Marmara Sea, and part of the submarine Izmit segment. Together they ruptured about 160 km of the fault system [20,40–42]. The 1912 Ms 7.4 earthquake ruptured the Ganos segment of the transform west of the Marmara Sea through the Gelibolu Peninsula and into the Gulf of Saros [21,43,44]. The 175 km segment of the NAF beneath the Marmara Sea has last ruptured in 1766 and is considered a seismic gap. Given the large accumulated slip and the stress increase caused by recent neighboring ruptures, the Marmara segment presents a high risk to the dense population around the shores, including the city of Istanbul [41,45,8,10].

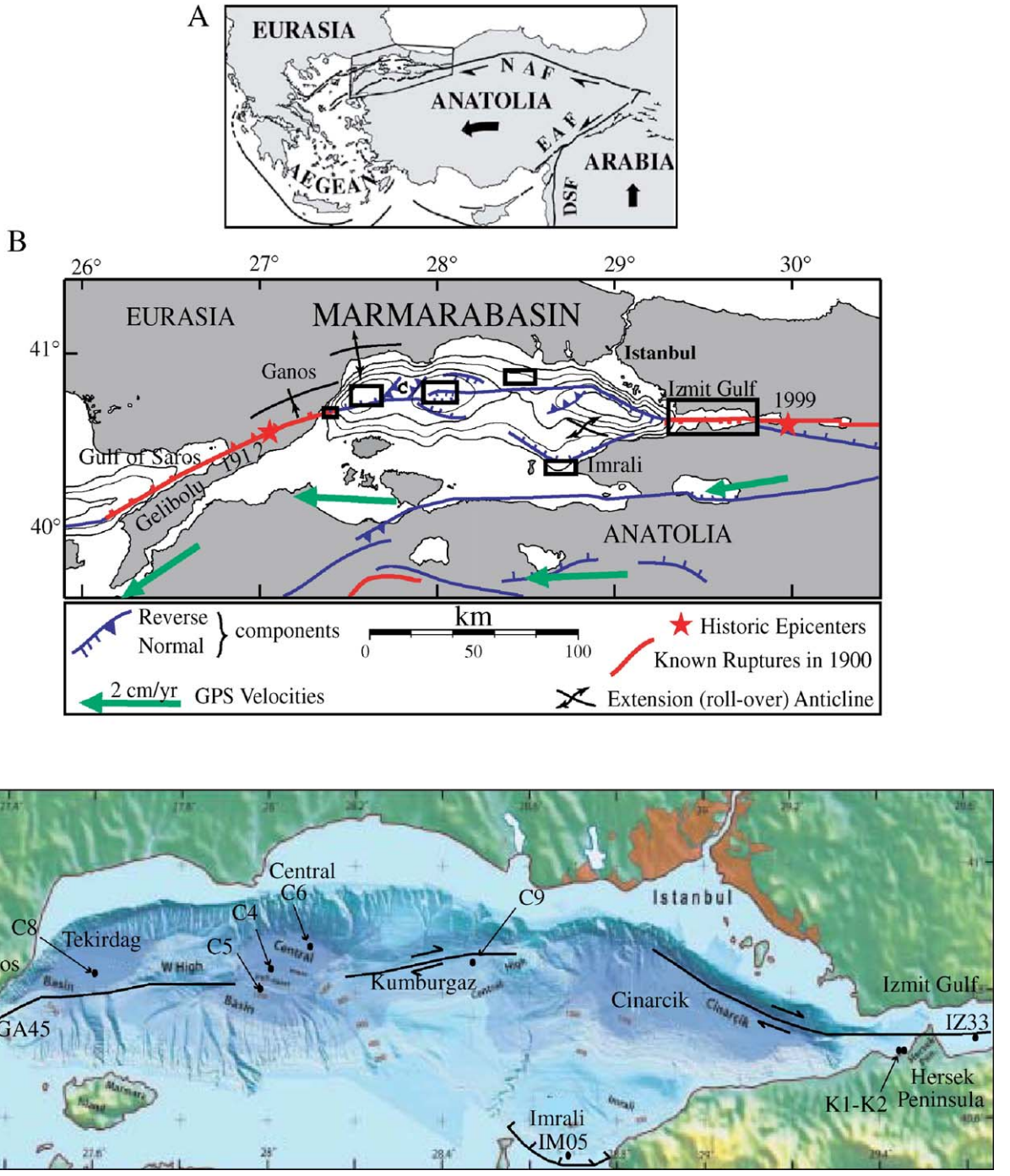

Fig. 1. (A) Tectonic interpretation of plate boundaries in the eastern Mediterranean region. Heavy arrows indicate the general direction of plate motion. NAF: North Anatolia Fault, EAF: East Anatolia Fault, DSF, Dead Sea Fault [33]. (B) Tectonic sketch of the Marmara Sea region (after [34]). Boxes mark the location of the basins studied from west to east: Ganos, Tekirdag, Central, Kumburgaz and Izmit Gulf. We also studied Imrali Basin along the southern shore of Marmara Sea. (C) Multibeam bathymetry of the Marmara Sea basins with some tectonic interpretation and location of studied cores. Modified after [29]. Image shows location of the larger transform basins: Tekirdag, Central, Kumburgaz and Cinarcik, and the location of the studied cores (GA45, C4–6, C8, C9, IM05, K1, K2, IZ33). The basins are ~ 1200 m deep and separated by saddles ~ 900 m deep. Kumburgaz is a shallower basin (900 m) located closer the shore. Cores C8 and C4 were located close to the basin depocenter.

1.3. Submarine earthquake geology

The evaluation of seismic hazards associated with faults and the understanding of fault mechanics in the brittle regime, critically depend on learning about the seismogenic evolution of the fault system through time. The historical record of major earthquakes along active faults rarely extends longer than the recurrence time of large earthquakes. Paleoseismology on land has contributed greatly to extend the earthquake record backward by identifying and dating their geologic signatures [46–49]. These signatures include features produced by fault motion along the rupture surface, as well as secondary structures derived from the shaking, such as landslides in the vicinity of the fault and liquefaction of sediments. Hence, earthquakes may be recognized as event-horizons in sedimentary sequences provided that sedimentation rates allow sufficient accumulation between events. Sequences of event horizons can be progressively deformed, thus providing a direct linkage between the tectonics and the earthquakes. Paleoseismic features include uplifted or subsided shorelines, drainage offsets, abrupt subsidence and/or uplift at pull-apart basins, compressional ridges, folding, tilting, fissuring and block rotation. Structural and stratigraphic relations can usually differentiate abrupt coseismic deformation from slow aseismic strain. Liquefaction features, slumps and tsunami deposits, are some of the secondary phenomena that characterize strong earthquakes. Earthquake geology has been widely applied on land to major continental faults over the past three decades (reviews in: [46–49]).

Tectonic activity does not end at the shoreline and with rapidly advancing submarine imaging and sampling technologies paleoseismology is beginning to develop in diverse submarine settings. For example, turbidites have been used as proxies for earthquake activity along the northern San Andreas Fault and at the Cascadia subduction zone where systems of canyons were cored and dated and the turbidites inferred to have been triggered by large earthquakes [13]. Earthquake generated turbidites and tsunamis have been documented in Sumatra [50], the Japan Sea [14], the Japanese Pacific coast [15], the California margin [16], Alpine lakes [51,52], New Zealand [48] and the Mediterranean an Marmara Seas [54,55]. Along the Dead Sea transform, a Holocene chronology derived from lake sediments provided an excellent record of its seismic history [56–59].

There are significant advantages to working in the submarine environment: (1) sedimentation is generally more continuous in time and in space than in onshore alluvial/fluvial settings, which are commonly characterized by hiatuses and extensive sediment reworking; (2) in isolated basins, sedimentation is likely to be free from the effects of weather and other non-earthquake-related events; (3) the calcium carbonate material of shells and the tests of microfossils can be effectively used for radiocarbon dating; (4) the short-lived radioisotopes contained in recent sediment yield precise chronologies for the past 150 yr; and (5) high-resolution geophysics can image the sea floor and subsurface with a resolution approaching the one obtained at an outcrop, but over much larger areas, thus permitting synoptic 3D views of the tectono-stratigraphic environment and a wide range of choices for sampling by precisely placed cores. While submarine earthquake geology relies heavily on the well established methodologies developed in land-based paleoseismology, results from the marine environment are likely to provide new insights in the seismogenic behavior of fault systems over the long term and thus open new opportunities for land studies and for studies of continental transforms in general.

2. Methods

High-resolution multibeam bathymetric mapping (ELAC1180 system) and subbottom chirp profiling (hull mounted Datasonics) conducted at 50 m spaced grids were obtained during two expeditions to the Marmara Sea with the *R/V Odin Finder* and *R/V Urania* in the fall of 2000 and summer of 2001, respectively [12,17,18]. Precise navigation was provided by differential GPS positioning and bathymetric maps were referenced to the WGS84 datum. Gravity cores (2–3 m long) and sediment water cores (SW-104) that leave an undisturbed sediment water interface were obtained in both expeditions. Similar cores recovered by the R/V Sismik-1 of the Mineral Research and Exploration Institute of Turkey (MTA) in the year 2000 were also analyzed (Fig. 1). The sediments in the cores were studied for grain size variability using a Sedigraph, and a sonic sifter, total organic carbon, calcium carbonate and for fine structures such as in turbidites by core radiographs. A chronology was established from ^{14}C derived from wood and foraminifers (Table 1) and from short-lived radioisotopes (^{137}Cs and ^{210}Pb). Radiocarbon dating was conducted at the National Ocean Sciences Accelerator Mass Spectrometry (NOSAMS) Facility at Woods Hole, MA, USA.

Marine species have depleted radiocarbon ages due: (1) to oceanic circulation processes that advect intermediate and deep ^{14}C depleted waters to the surface, (2) atmospheric ^{14}C changes and (3) air–sea CO_2 exchange

Table 1
Radiocarbon age ranges in years AD calibrated with Calib. 5.0.2 [64]

Sample	Type	14-C age	±1 sig.	AD calibrated age ranges				Most prob.	Sample location
				Calib. ΔR	1σ	Lower	Upper		
C4, 45 cm	Forams	1040	70	81±40 [a]	1	1333	1432	1390	Above
C4, 155 cm	Forams	1640	35	81±40	1	702	916	822	Above
C4, 244 cm	Forams	1760	35	81±40	1	606	820	715	Below
C4, 244 cm	Forams	2930	90	81±40	1	−774	−544	−646 [b]	Below
C8, 55 cm	Forams	1320	105.9	81±40	1	1053	1248	1019	Above
C8, 65 cm	Forams	1460	148.7	81±40	1	865	1177	1157	Below
K2, 28 cm	Bivalve	550	50	81±40	1	1832	1950	1860	Above
K2, 38 cm	Gastropod	590	60.2	81±40	1	1717	1884	1816	Above
K2, 39 cm	Bivalve	795	60.2	81±40	1	1532	1652	1588	Above
K2, 63 cm	Mollusk	725	98.5	81±40	1	1536	1730	1548	Below
K1, 65 cm	Bivalve	845	50	81±40	1	1489	1595	1542	Below
GA45, 42 cm	Wood	Mod							Within
GA45, 81 cm	Wood	Mod							Within
GA45, 88 cm	Wood	Mod							Within
Calib. curve									
GA45, 113 cm	Wood	30	95	intcal04	1	1810	1922	1828	Below
IZ33, 203 cm	Wood	1200	40	intcal04	1	777	882	824	Within
IZ33, 262 cm	Wood	1830	45	intcal04	1	130	236	182	Within

Most prob. refers to the most probable age. The location of each sample is described relative to the interpreted seismite event (above, below, within). Those samples within the event were obtained from woody material recovered from the basal part of the seismite.
[a] The marine reservoir correction was obtained from [61] by averaging values obtained to the north and south of the Marmara Sea.
[b] Negative numbers indicate cal BC ranges.

processes [60,61]. Reservoir ages of the global mixed marine surface layer, atmospheric ^{14}C changes and air–sea CO_2 exchanges have been calculated for the world's oceans [62,63,60]. However, deviations (ΔR) to the marine reservoir ages in response to local oceanic conditions must be accounted for. We calibrated the ages to calendar years with the CALIB 5.0.2 program [64] and applied a marine reservoir correction for the Marmara Sea of 460+40 yr (ΔR 71) and 340+40 yr (ΔR 91) obtained from AMS ^{14}C dates of modern pre-bomb mollusk shells [61]. We applied a weighted mean ΔR 81 (by averaging both ΔR deviations) with a standard deviation of 14.1 and a mean measurement error of 28.3 and assigned the most statistically probable age to a deposit [64].

Gamma counting for short-lived radioisotopes was conducted at Lamont-Doherty Earth Observatory of Columbia University. The ^{137}Cs chronologies reveal both the 1986 Chernobyl release peak and the 1965 nuclear testing global fall-out. These chronologies are very useful to date the core tops [65–67]. The ^{210}Pb chronology with a half-life of 22.3 yr permits to date the sediment back for 150 yr [68–70]. ^{210}Pb can be both in supported and unsupported forms. In this study we use the unsupported ^{210}Pb derived from the atmospheric decay of ^{222}Rn and referred to as excess ^{210}Pb. Supported ^{210}Pb also forms in the sediments from the decay of ^{226}Ra but it is in equilibrium with previous decay chain members and does not provide a chronology. Once the chronology of a homogenite or mass-wasting event was established, the sedimentary deposit was declared a "seismite" if it correlated in time and space with a large earthquake in the historical record [71,72].

3. Results

3.1. The Marmara Sea as a natural laboratory

The Marmara Sea constitutes an excellent setting for developing and testing methodologies for submarine earthquake geology from earthquake ruptures because the seismic history of the region has been documented for nearly 2000 yr [19–23]. The Marmara Sea is a transtentional structure composed of three main transform basins, from east to west: Cinarcik, Central and Tekirdag, with water depths of 1200 m, and separated by ridges 700 to 900 m deep [29,30,73] (Fig. 1). These basins probably contain Pliocene and Quaternary strata 1–4 km in thickness with most of the sedimentary infill being of terrigenous and lacustrine origin [74–77]. The Marmara Sea also contains intermediate size basins in Izmit Gulf, a 50 km-long EW-oriented coastal inlet [78,79,18]. The basins are: the Western Basin (also

known as Darica Basin), the Central Basin (also known as Karamürsel Basin) and the Eastern Basin (also known as Golcuk Basin). Each basin is 10–20 km long, 5–9 km wide and 40–220 m deep. These basins are separated by two shallow sills located north of Hersek Peninsula (54 m deep) and north of Golcuk (33 m deep) [18]. Smaller basins on the western Marmara Sea shelf (1 km in diameter and at 100 to 150 m of water depth or less) are found associated to the Ganos segment of the North Anatolia Fault. This paper addresses the Holocene sedimentary record of the Marmara Sea in two of the main basins, in two intermediate size basins in Izmit Gulf and one of the small basins along the Ganos Fault. Despite differences in size, these basins share interesting characteristics in their sedimentation patterns, which we ascribe to earthquakes. Coseismic effects of large sea-floor rupturing earthquakes, including permanent deformation along the fault and shaking, are dominant factors for the infilling history of the basins.

3.2. Earthquake signature in small transform basins

The Holocene record of the Ganos segment of the NAF was surveyed about 2 km away from the shoreline

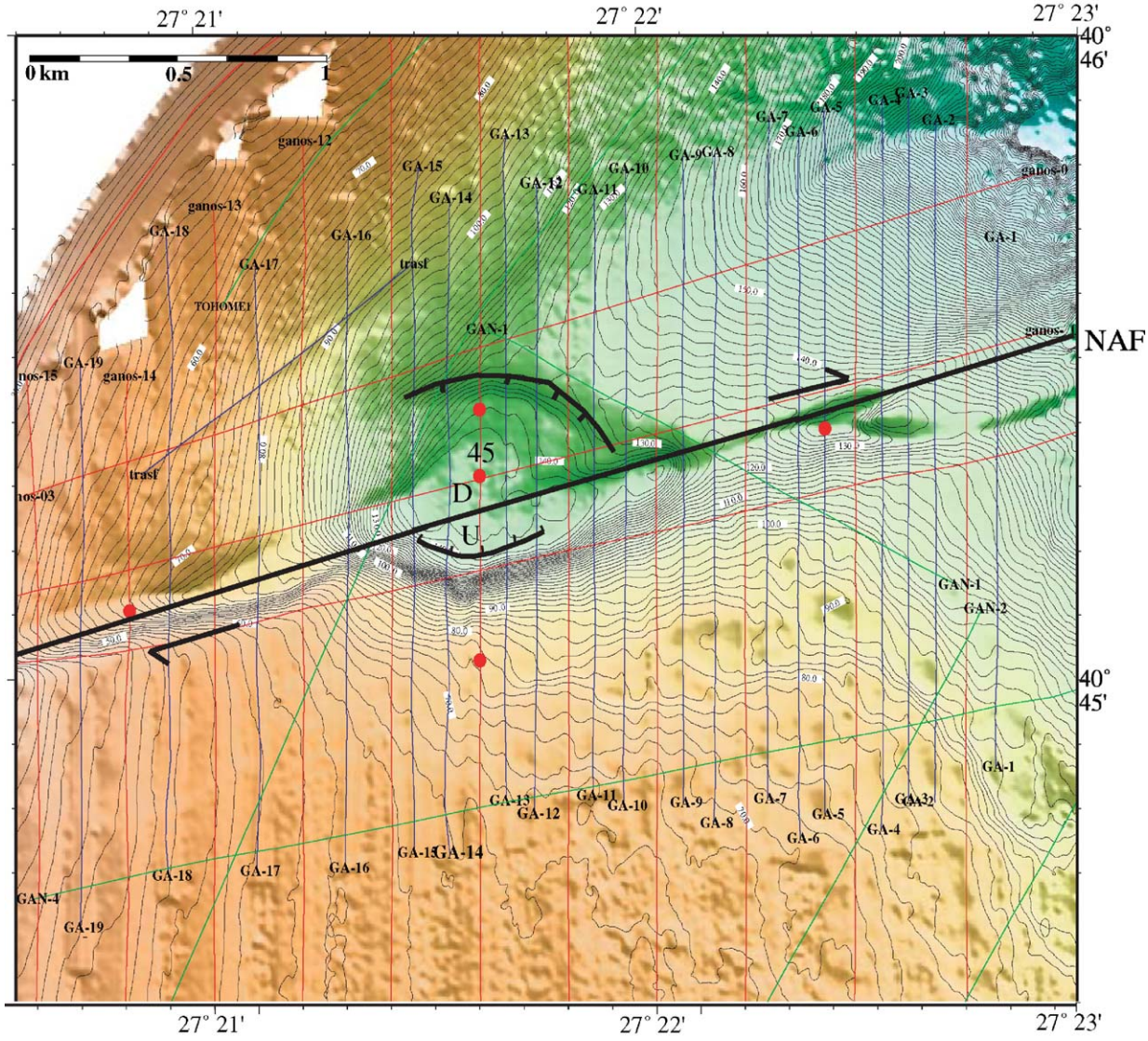

Fig. 2. High-resolution multibeam bathymetry (2 m contour interval) showing the path of the NAF across the shelf. The NAF bisects the 40 m deep Ganos small transform basin. The shoreline is 2–4 km away. Red dots show location of cores and lines mark subbottom profile tracks. Also shown the interpretation of normal faulting [34].

and 40 km from the 1912 earthquake area of maximum disruption on land. The sea-floor expression of the NAF across the shelf and slope (from 35 to 150 m of water depth) is manifested by a deep (15 m), narrow (100 m) furrow that opens into a circular basin 1 km in diameter, 40 m deep, followed by a smaller elongated basin (100 m wide, 300 m long, 10 m deep; Fig. 2). Further east, mass-wasting obscures the fault trace across the slope leading to the Tekirdag Basin. The westernmost and largest basin, informally named here Ganos Basin, has a steep (30°) southern wall covered by 5 m of Holocene hemipelagic sediments and a less steep northern wall (14°) draped with at least 20 m thick Holocene sediments. The NAF bisects the Ganos Basin. Kinematics on this portion of the NAF is transtensional and the basin is thought to be controlled by a shallow-rooted listric border fault closely coupled with the main branch of the NAF [34].

The floor of the Ganos Basin is underlain by a characteristically intercalated sequence of sand-rich layers that fine upwards and mud (Figs. 3 and 4). The sand-rich layers are initiated by a sharp basal erosional contact that is overlaid by multiple millimeter to centimeter thick laminae of fine-grained sand and coarse silt that grade into a thick wedge of homogenous medium- to fine-grained silt. These fining-upwards sequences tend to have a higher percentage of total organic carbon content (up to 2.5% TOC) than the pelagic sediments (1.5% TOC) and are separated from each other by thin beds of foraminifera-rich clay (average 5 cm). These sand-rich deposits are analogous to "homogenites" first described for the Mediterranean Sea [80] as an acoustically transparent unit characterized by an erosional base and a series of sandy layers that fine upwards. The homogeneous sediment associated to these deposits tends to be thicker than the sand and silt beds and therefore the deposits are called homogenites even though they contain coarse-grained beds and laminae. Homogenites have been associated to earthquakes and tsunamis in several tectonic setting [80–82,51–54] and were recently described for Central Basin of the Marmara Sea [83].

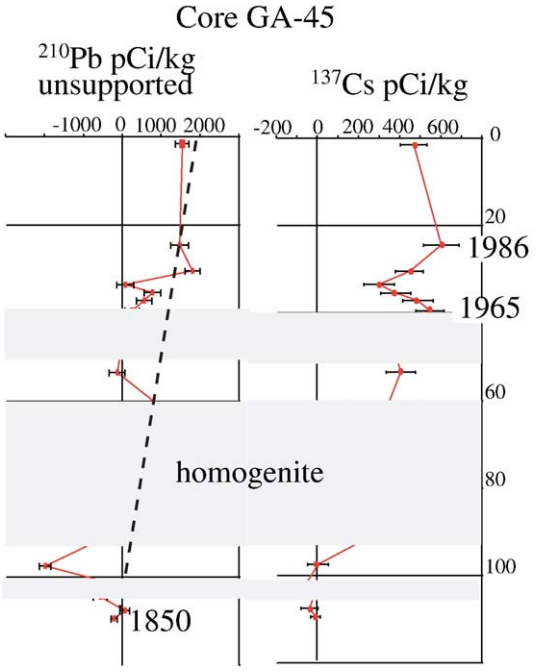

Fig. 3. ^{210}Pb and ^{137}Cs short-lived radioisotope chronology of core GA45. The core was recovered with an undisturbed sediment water interface near the center of the large Ganos Basin. The upper 40 cm of the core are not reworked and the ^{137}Cs counts permit to resolve the 1965 global fall-out peak due to nuclear testing and the 1986 Chernobyl nuclear reactor event. The ^{210}Pb chronology is not well resolved due to sediment reworking. A radiocarbon age of 1850 (with large error bars) at 110 cm tentatively marks the ^{210}Pb decay.

This study provides evidence for homogenite deposition in the Marmara Sea that can be directly linked to historical earthquakes in Ganos, Tekirdag and Central Basins. In the Ganos Basin, we identified three homogenites that have tentatively been correlated to regional historic earthquakes: the large 1912 rupture across the Gelibolu Peninsula and into Saros Gulf and the smaller 1965 and 1859 events confined to the Gulf of Saros, 60 km away (Figs. 3 and 4). The 1912 Ganos homogenite can be traced on the chirp profiles throughout the basin floor as a thick deposit (~3 m) that truncates subparallel seismic reflections near the southern margin of the basin (Fig. 5). Core 45 sampled the thinner edge of the deposit to the north (Fig. 5). The homogenite deposit overlays folded and offset seismic reflection surfaces at the fault trace. These disrupted reflectors are interpreted as the 1912 earthquake rupture on the floor of the basin. We therefore classify the event as a "seismite" (i.e.,[84,85]). The land rupture was mapped from the shoreline, 5 km westward from the Ganos Basin, for 40 km across the Gelibolu Peninsula to the area of maximum reported damage. A lobate feature beneath the 1912 homogenite deposit is interpreted as a mass-wasting event that was subsequently disrupted by the earthquake and was probably generated by an older event. An age model for the upper 50 cm of undisturbed sediment indicates average linear sedimentation rates of 0.5 to 1.0 cm/yr (Fig. 4). Tectonic subsidence is likely to be even faster otherwise the 40 m deep young basin would have been filled by sediment in approximately 8000 to 4000 yr.

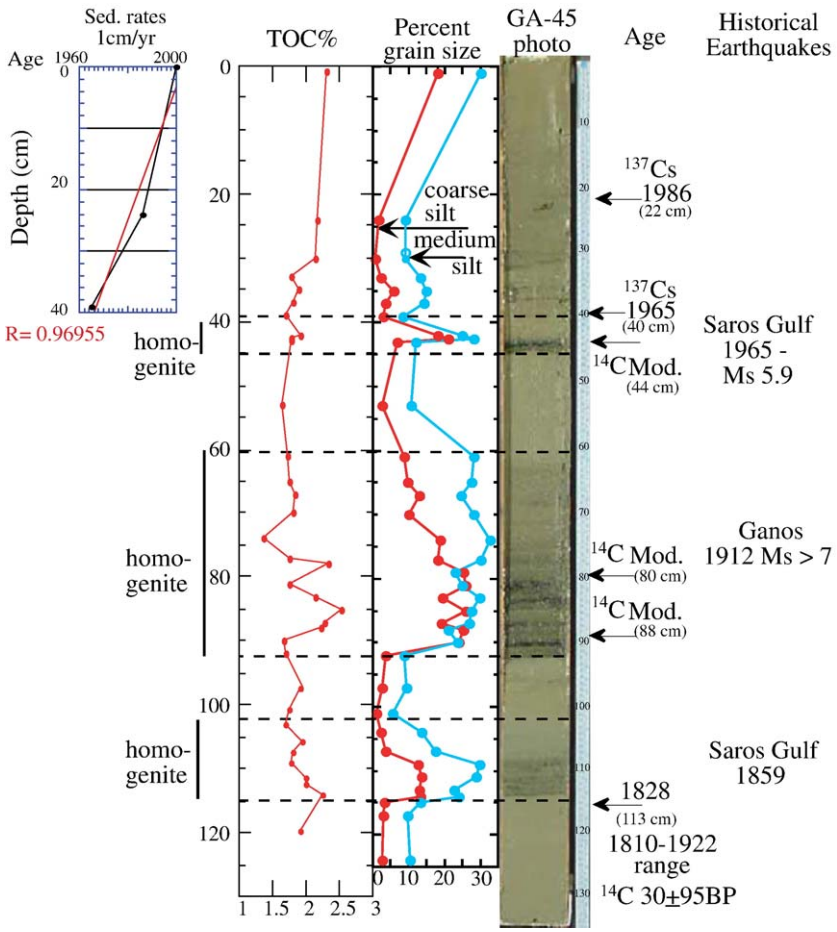

Fig. 4. Grain size variability ranging from fine-sand to fine-silt and an increase in the total organic carbon of the sediments (TOC %) permit to resolve three homogenite deposits (40–44 cm, 60–92 cm, 100–112 cm). The homogenites are initiated by a sharp basal contact overlaid by multiple sand- and silt-size laminae that fine upwards to a thick wedge of homogenous fine-grained silt. The homogenites are separated by thin beds of clay (5–10 cm). Short-lived radioisotopes and radiocarbon chronology permit to construct an age model for correlation of the homogenites to the historical record of earthquakes: the large 1912 Ganos event Ms > 7 that lead to the deposition of a 30 cm thick homogenite and two smaller events that occurred in the Gulf of Saros. Sedimentation rates of 1 cm/yr were calculated for the upper 40 cm of the core that is apparently undisturbed.

3.3. The long term earthquake record of the deep transform basins

The largest and deepest basins in the Marmara Sea as well as all of the basins studied in this work are associated with the northern branch of the NAF. Structurally, most basins in the Marmara region are located on the releasing side of bends on strands of the transform [29,86,34]. In order to account for the extension, these fault segments are typically non-vertical and slip obliquely with dip-slip components that decrease away from the bend. They thus serve as border faults of oblique half grabens that tilt toward the fault and toward the bend. Consequently, these basins are typically triangular with depocenters at the narrow and youngest end of the basins near the fault at the bend [34]. The structural evolution of these transform-bend-related basins is most likely preserved in the sedimentary record of their depocenters and represented a critical target in our coring strategy.

Sediments were recovered from cores near the depocenters of Tekirdag and Central Basins (~1200 m) and from a smaller and shallower (900 m) Kumburgaz Basin (Fig. 1). The major goal was to test whether the basins contained a record of all large-scale earthquake events that occurred within the Marmara Sea region with Ms > 7 and to identify the signature of these events in the stratigraphic record. We concentrated our efforts in cores recovered near the depocenters because analyses (grain size, TOC, calcium carbonate) showed that cores recovered near the slope and in the shallower Kumburgaz Basin are composed mostly of reworked sediment

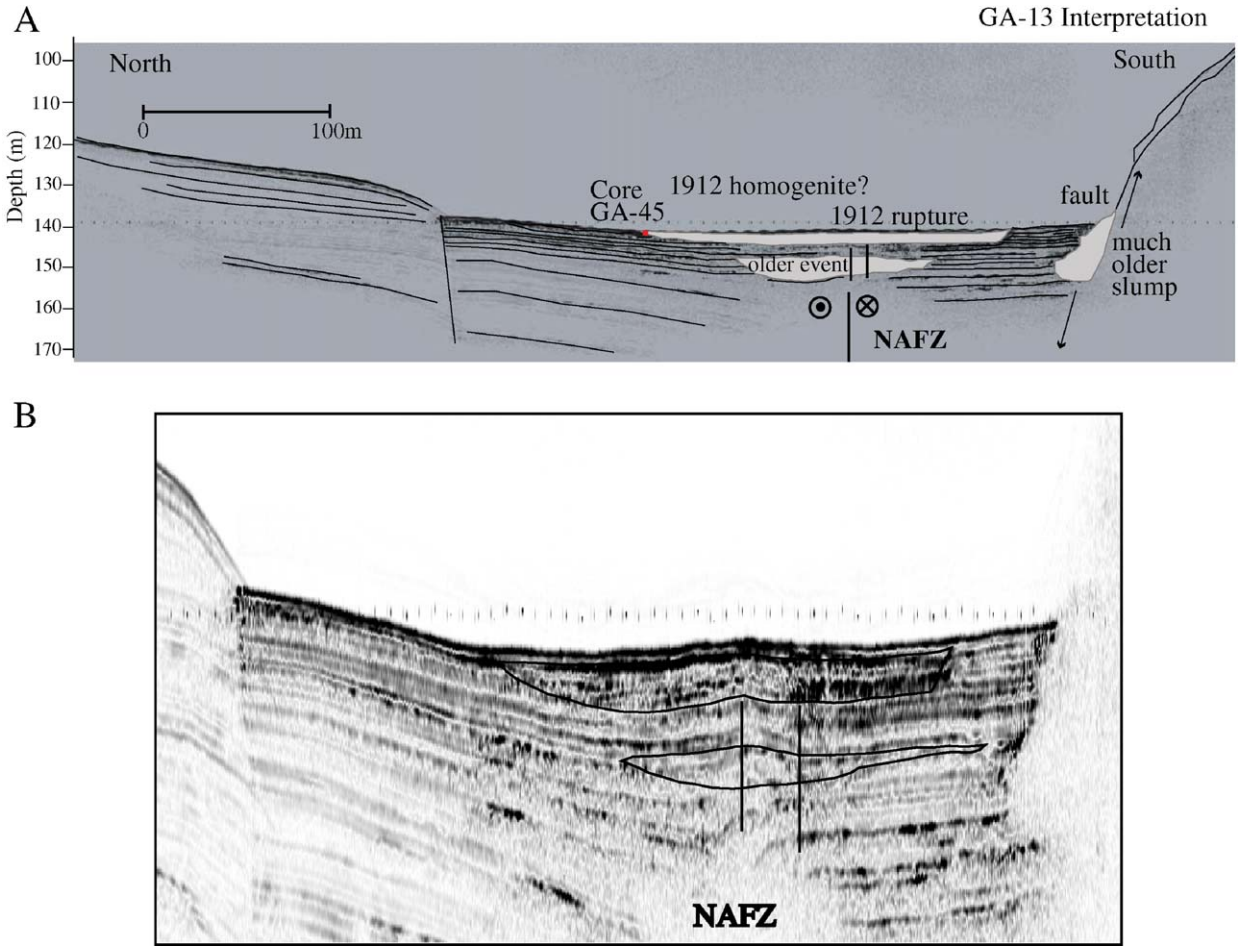

Fig. 5. (A) Subbottom CHIRP profile GA13 across the large Ganos Basin showing location of core GA45. Correlation of the subbotttom profile to the lithology indicates that the core recovered the thin edge of a much larger and thicker (3–5 m thick) homogenite and/or mass-wasting deposit that extends throughout the basin floor truncating seismic reflectors towards the southern part of the basin. We interpret the homogenite/mass-wasting deposit and the disrupted and off-set seismic reflectors beneath as sea-floor ruptures related to the 1912 earthquake event. A lobate deposit beneath is interpreted as an older event indicating that these basins may contain a record of local fault ruptures. The NAFZ bisects the basin. (B) Close-up of the 1912 homogenite/mass-wasting deposit vertically disrupted and possibly folded strata beneath, and older event.

and contain numerous turbidites that were probably derived from climatic events such as floods and shelf downslope transport, thus complicating the identification of earthquake-related events [87,88]. These turbidites are normally graded but differ from the homogenites in that they are thin-bedded (average 1 cm thick), do not contain multiple laminae, and are not capped by a wedge of homogeneous sediment. In contrast, the cores recovered near the depocenters of Tekirdag and Central Basins contain homogenites that can be correlated to the historical record of earthquakes in both basins (Fig. 6).

The basal part of the 3 m long cores contains sediment layers about 10 cm thick, dark green to black and with average total organic carbon content (TOC) of 1% (Figs. 7 and 8). These layers are iron-rich but can also be interpreted as sapropelic, meaning layers of similar color and thickness as sapropels but that contain less TOC, from 0.5% to 2%. Sapropels were identified in the Marmara Sea as phosphorescent green to gray sediments having >1 cm in thickness and >1.5% TOC [89]. We obtained a radiocarbon age of 2930 BP above the iron-rich layers, indicating that they are slightly younger than the youngest sapropels dated 3500 ^{14}C yr BP [89] (Table 1). In Central Basin, the sediment above the iron-rich layers contains two homogenite deposits separated by beds of clay only a few centimeters thick and with abundant foraminifers. These foraminiferal-rich layers are interpreted as undisturbed pelagic sedimentation and provide the ^{14}C chronology needed

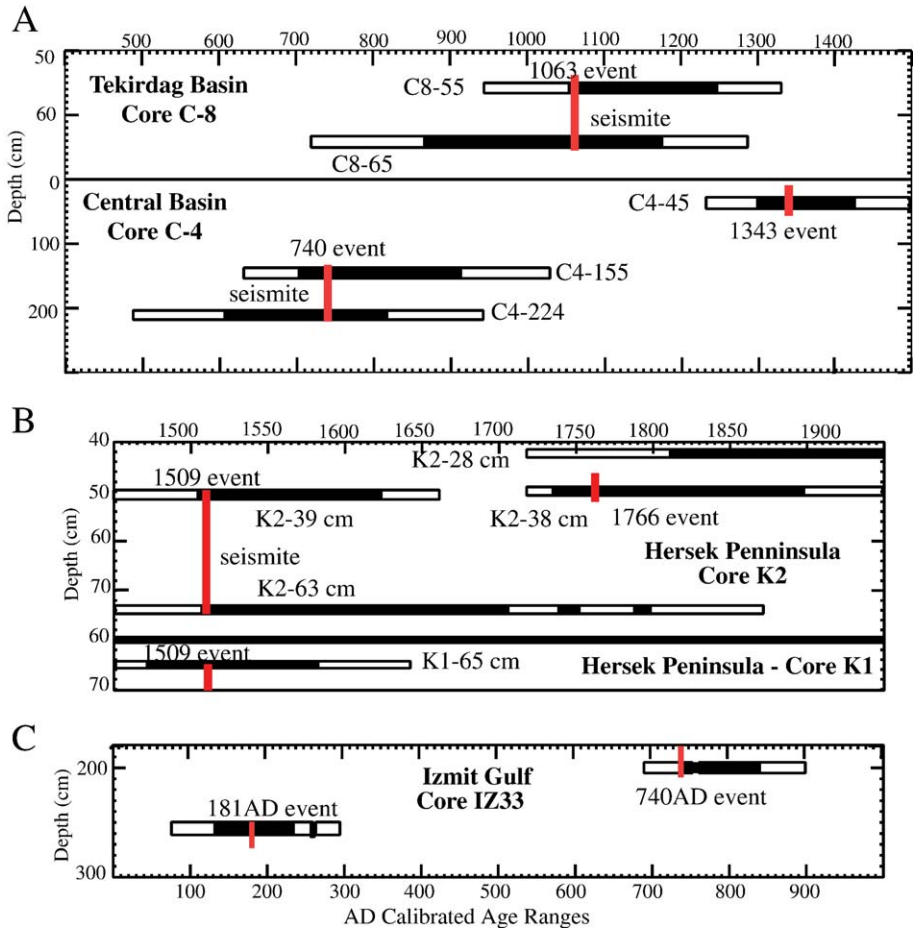

Fig. 6. Calibrated ages to AD ranges. Plots show error bars based on Calib. 5.0.2 program [61–64]. The *y*-axis shows the depth in a core, the *x*-axis the calibrated years. The red lines indicate an earthquake event. (A) Tekirdag and Central Basins, (B) Hersek Peninsula, (C) Izmit Gulf. (For interpretation of the references to colour in this figure legend, the reader is referred to the web version of this article.)

to correlate the homogenites to the 740 AD and 1343 earthquakes [19–23] (Table 1, Figs. 6 and 7). In Tekirdag Basin, we documented from the grain size variability and inverse stratigraphy (old over young) several intervals of reworked sediment above the iron-rich layers (Fig. 8). One of these deposits has been tentatively correlated to the 1063 historical earthquake (Figs. 6 and 8, Table 1). The upper 50 cm of both cores are within the reach of both ^{137}Cs and ^{210}Pb chronology and reveal both the 1986 Chernobyl release peak and the 1965 nuclear testing global fall-out (Figs. 7 and 8, [65–67]). The chronology derived from short-lived radio-isotopes and sedimentation rates calibrated to the stratigraphy in both Tekirdag and Central Basin cores show a sharp discontinuity at ~30 cm interpreted as an erosional event. This event can be correlated in both basins to the 1912 earthquake. However, more cores are needed to characterize the 1912 event more precisely in Tekirdag and Central Basins. Generally, event-horizons associated with earthquakes exhibit both erosion and deposition. This kind of mixed response may characterize cores that sample the 'basin floor, but not necessarily the current slope-less depocenter where gravity flows such as homogenites are ultimately transported and deposited.

3.4. The record of recent earthquakes west of the Hersek Peninsula

The Gulf of Izmit west of the Hersek Peninsula was surveyed for evidence of Holocene faulting and three cores K1, K2 and K3 were recovered at water depths of 35 m (Fig. 9). All three cores contain a mass-wasting deposit at about 40 to 60 cm below the sea-floor (Fig. 9). The deposit is composed of coarse sand in a muddy matrix with floating clay clasts and *Turrietela* sp. (a

gastropod of shallow water affinity). The basal contact is a pronounced scour surface. Core K2 is fractured from the base of the sandy mass-flow at 60 cm to about 20 cm below the surface. Radiocarbon ages obtained from mollusks above and beneath the sandy mass-flow were correlated to the historical record of earthquakes and show evidence of two possibly three events. The basal part in both cores K1 and K2 correlates with the 1509 earthquake (Figs. 6 and 9). The upper part of the sandy mass flow correlates with the 1766 earthquake. The fracture is younger than 1860 and could have resulted from the 1894 earthquake, which devastated the coastal region from the Gulf of Izmit to the northeast side of the Marmara Sea [20]. Core K2 has a complex stratigraphy that we interpret as mixing and reworking of the deposit by two events and younger fracturing.

3.5. Sediment erosion linked to earthquakes in the gulf of Izmit

The stratigraphic record of the Gulf of Izmit provides information about the processes that dominate the sedimentation of submarine transform basins. The central basin has a narrow southern shelf, a broad northern shelf and two subbasins (Figs. 9 and 10). The floors of the subbasins are flat and subbottom profiles show that seismic horizons are progressively tilted toward the fault and are truncated opposite to the fault and onlap the fault (Fig. 10). Commonly, an acoustically transparent layer that extends across the basin overlies these truncated reflectors. Correlation of seismic images to the lithology and chronology derived from the cores shows that the truncated seismic horizons correspond to scour surfaces overlaid by medium to coarse-grained sand beds that are 5 to 10 cm thick. These sandy deposits are separated by intervals of homogeneous mud that we interpret to correspond with the acoustically transparent horizons on the chirp records. Two such events were dated by radiocarbon and the calibrated ages were correlated with the 181 AD and 740 AD earthquakes [19–23]. The upper meter of the core contains a mass-wasting deposit near the top that could potentially have resulted from the 1999 Izmit and/or Duzce earthquakes, but the core was not available for dating. Lack of a more complete record of historical earthquakes in Izmit Gulf is again ascribed to incomplete sampling of the depocenter areas.

3.6. Vertical motion along the Southern Boundary Fault

One of the major goals of the research was to use high-resolution bathymetry and subbottom profiles coupled to sediment data to quantify fault motion; both strike-slip and vertical components. The Marmara Sea consists of a series of semi-isolated basins that are separated by sills and offers an ideal set of reference horizons. During the late Pleistocene–Holocene glacial cycle when global sea-level dropped below the 87 m Dardanelle's Sill, Marmara was isolated from the global ocean and became a fresh-brackish water lake [90,91,76,77]. As such the paleoenvironments of deposition (rivers, estuaries, deltas, beaches), faunal (mollusks, foraminifers, ostracods) and floral (diatoms, pollen) assemblages changed from marine to brackish-fresh water and to marine providing excellent time markers. We surveyed the Imrali shelf along the Southern Boundary Fault and the acoustic images clearly show footwall collapse and an active normal fault scarp (Fig. 11). Surficially, fault activity is manifested by a series of rotational slumps concave towards the basin. The steep slope that is created by the active normal fault, however, probably triggers these slumps. Core IM05 was recovered from 150 m of water depth at the base of one of these scarps (Fig. 11). The sediments, floral and faunal assemblages in this core recorded the transition of the Marmara brackish lake to the Marmara Sea and provided indicators of paleowater depths [92]. Calibrated radiocarbon ages provided an age of 14.0 ka BP for the marine flooding of Marmara Lake [92].

Based on the chirp records we were able to measure a vertical offset of 30 m by tracing seismic reflections (Fig. 11). Fifteen meters of footwall collapse were quantified along a fresh looking scarp. Fifteen meters of vertical offset are attributed to a receding normal fault scarp. A fault scarp that increases in height due to fault slip can explain the mechanism for failure. The footwall fails progressively further from the original fault, thus effectively shallowing the dip of the upper portion of the fault. This type of failure is expected if the fault surfaces in weak strata as the Miocene–Pliocene clay-evaporite formation that outcrops nearby the Imrali shelf on the north side of the Armutulu Peninsula. Based on the 14.0 ka BP age determined for the marine flooding surface, a rate of 1 mm/yr was calculated for the 15 m of vertical displacement due to footwall collapse. Possibly an additional 1 mm/yr could have resulted due to the receding normal fault scarp. After reconstruction of 30 m of vertical offset due to faulting processes, core IM05 is at −120 m of water depth and the paleoshoreline at −95 m possibly as deep as −120 m (Fig. 11). This means that, at the time of the marine flooding, core IM05 was at paleowater depths of approximately −35 m and the paleoshoreline was at a depth of −8 m below the

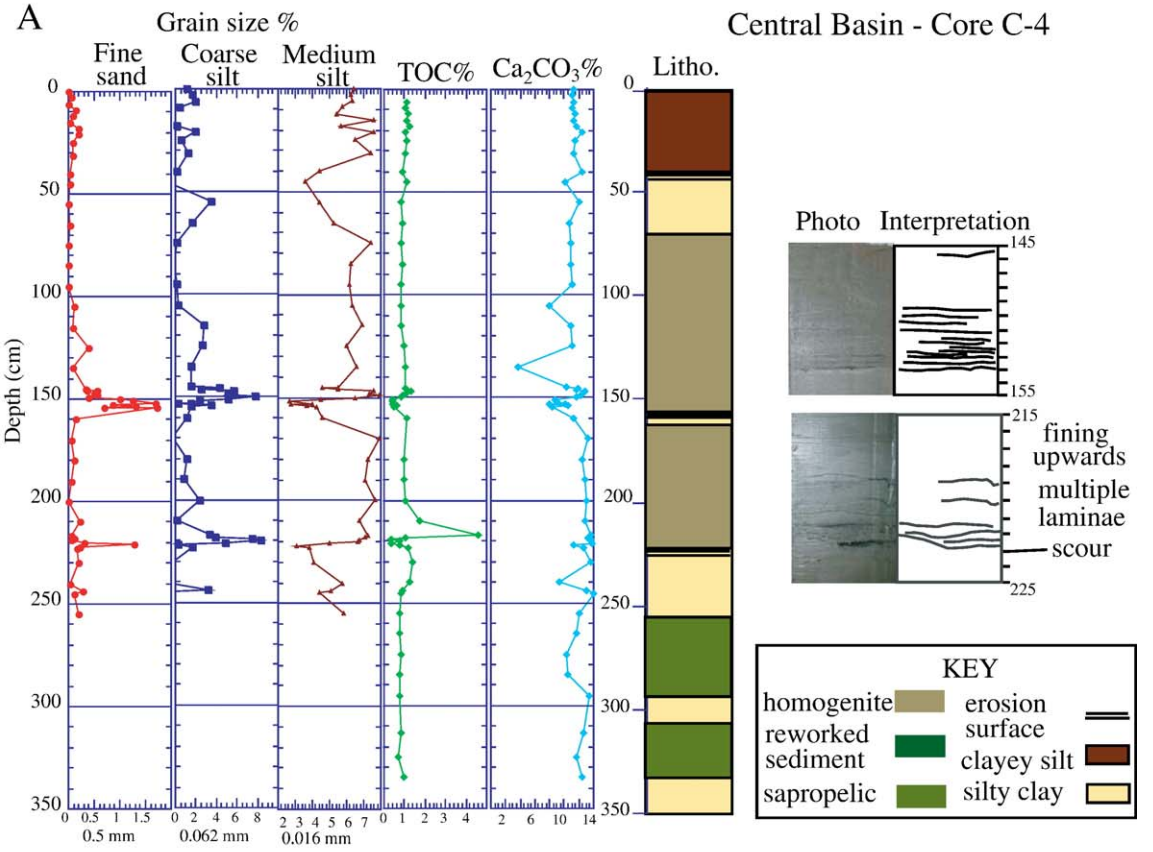
A
Grain size %
Central Basin - Core C-4
Fine sand
Coarse silt
Medium silt
TOC%
Ca_2CO_3%
Litho.
Depth (cm)
0.5 mm
0.062 mm
0.016 mm
Photo
Interpretation
fining upwards
multiple laminae
scour
KEY
homogenite
reworked sediment
sapropelic
erosion surface
clayey silt
silty clay

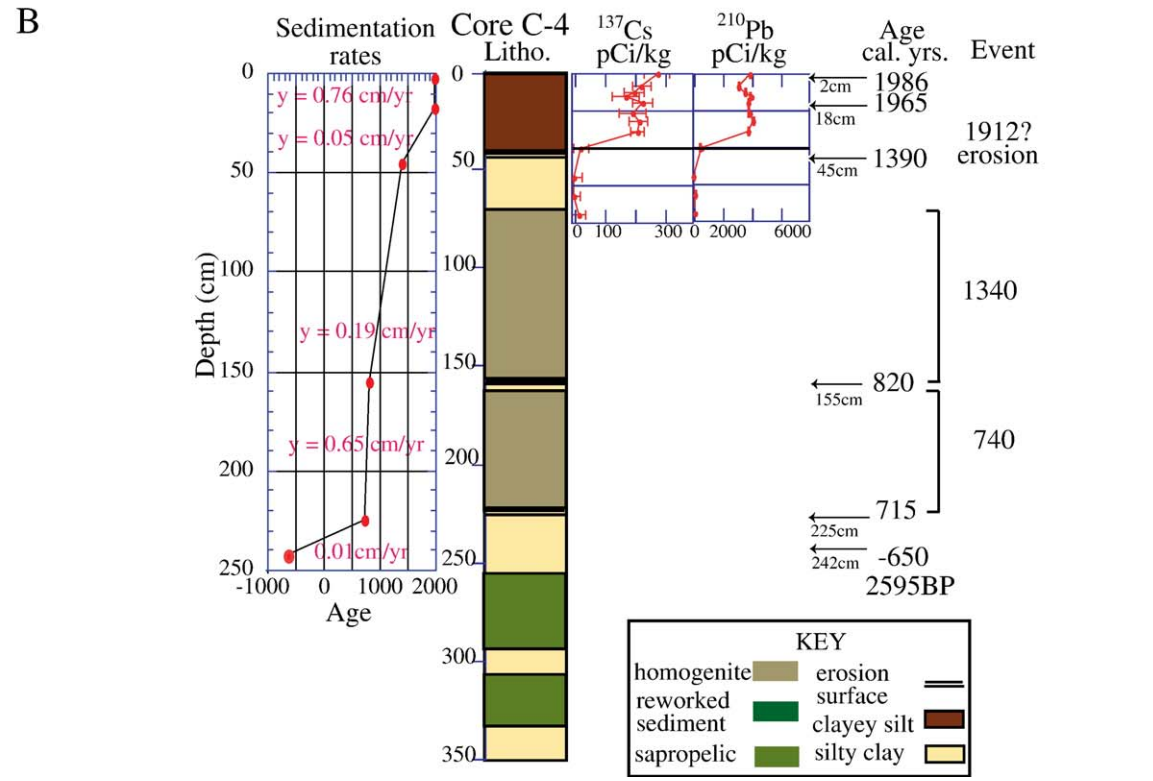
B
Sedimentation rates
Core C-4
Litho.
^{137}Cs pCi/kg
^{210}Pb pCi/kg
Age cal. yrs.
Event
y = 0.76 cm/yr
y = 0.05 cm/yr
y = 0.19 cm/yr
y = 0.65 cm/yr
0.01cm/yr
Depth (cm)
Age
2cm
1986
18cm
1965
1912?
45cm
1390
erosion
1340
155cm
820
740
225cm
715
242cm
-650
2595BP
KEY
homogenite
reworked sediment
sapropelic
erosion surface
clayey silt
silty clay

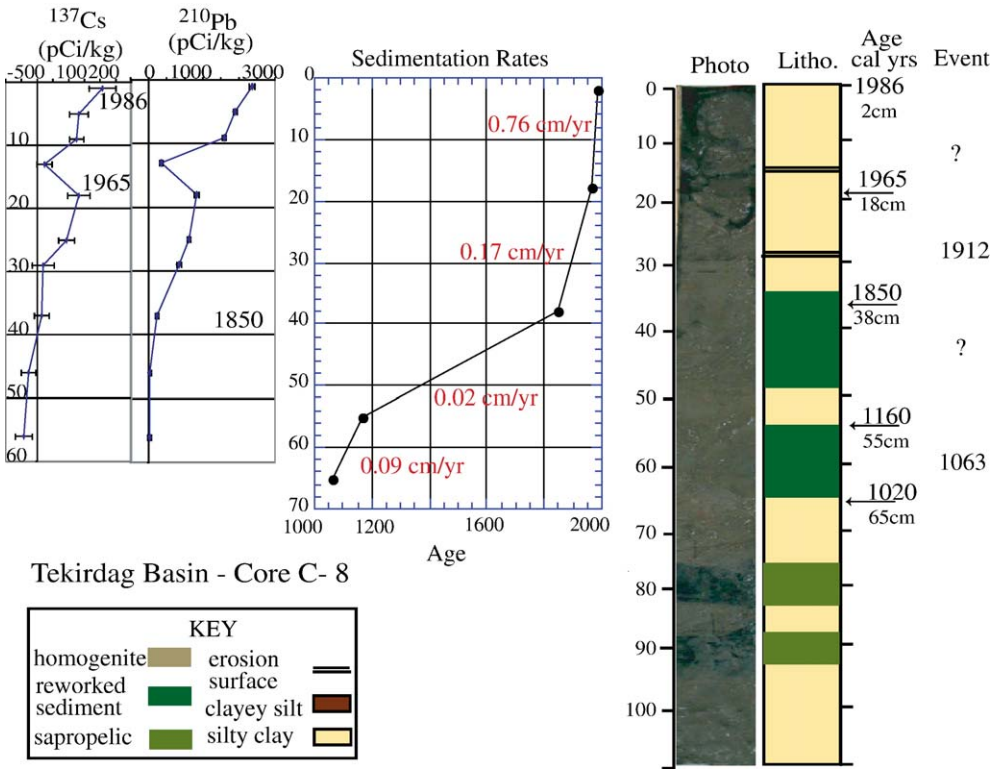

Fig. 8. Core C8 from Tekirdag Basin. Short-lived radioisotopes, sedimentation rates, photo, lithology and radiocarbon age (in calendar years) permit to identify several intervals of reworked sediment. The event bracketed between 65 and 55 cm has been correlated to the 1063 historical earthquake. A surface at 30 cm is related to the 1912 event.

Dardanelles outlet sill and possibly as low as −35 m. This paleowater depth is consistent with paleoshorelines present along the northern and eastern shelves that lie below the level of the Dardanelles outlet sill of −87 m and suggest a drawdown of Marmara Lake prior to the marine flooding [93]. These findings are also consistent with the fauna contained in the lake stage of Core IM05 because the *Dreissina rostriformis* banks recovered from the core thrive in water depths of 0 to −35 m (Fig. 11) [94,95].

4. Discussion

4.1. Submarine earthquake geology in transform basins

Small transform basins such as the Ganos Basin along the NAF are excellent paleoseismic sites to document earthquake ruptures specific to those fault segments and to compare the structural effects of earthquakes (e.g., strata offsets and truncations) with sedimentation effects (e.g., homogenites, mass-wasting deposits). First, these isolated basins intersect the fault trace and record preferentially local processes including earthquake ruptures, sediment failures and resuspension. In the Ganos Basin correlation of the stratigraphic data to the geophysics provided a powerful tool that permitted to map the 1912 earthquake rupture and seismite. Furthermore, the data suggest that deeper mass-wasting deposits may be related to older ruptures. Longer cores should permit to resolve this issue in the future. The Ganos Basin is 60 km away from the Gulf of Saros; therefore, it is not surprising to find the sedimentary effects of earthquakes associated to the Gulf of Saros in its stratigraphic record. However, the homogenites correlated to the Gulf of Saros earthquakes are not associated to sea-floor deformation and rupture

Fig. 7. (A) Core C4 recovered near the Central Basin depocenter: grain size, total organic carbon and calcium carbonate percentages, lithology, photo and interpretation permit to identify two homogenites. (B) Sedimentation rates are fast (0.1 to 0.76 cm/yr) within the interpreted homogenite deposits and near the top. The age derived for short-lived radioisotopes and radiocarbon calibrated to years AD permits to link the homogenites to the 740 AD and 1340 AD events. An erosional surface is possibly related to the 1912 event.

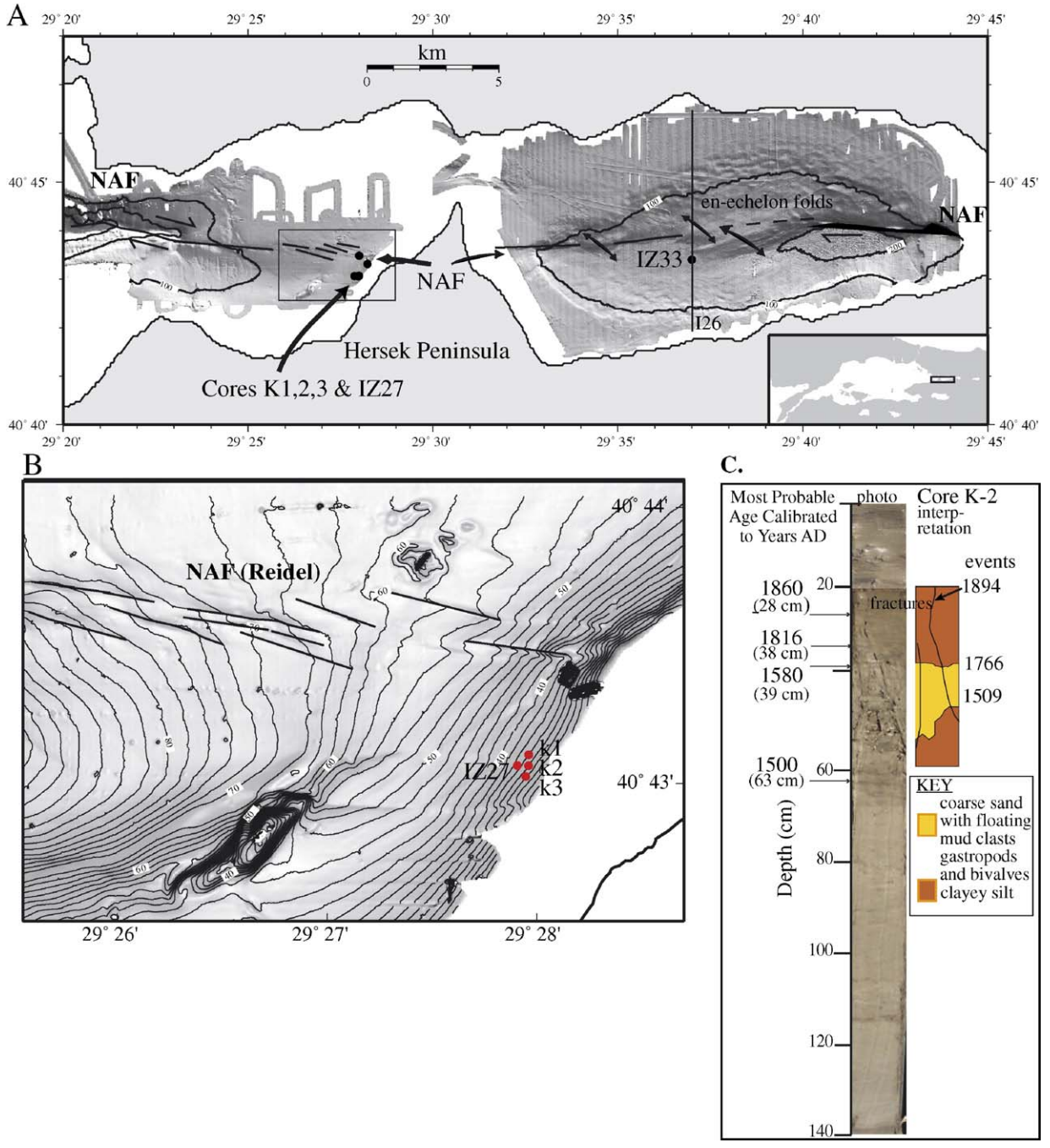

Fig. 9. (A) Multibeam bathymetry of Izmit Gulf, Central Basin, also called Karamursel Basin, Hersek Peninsula and part of the Western Basin [18]. Also shown location of studied cores, the North Anatolia Fault, Reidel faults and three en-echelon folds associated to the NAF. (B) Close-up of box shown in "A" with bathymetric contours and core locations. (C) Calibrated ages, photo, lithology and historical earthquake events of core K2.

as the 1912 seismite. Second, these young basins are tectonically very active. The sedimentation rate in the Ganos Basin was calculated at 0.5 to 1.0 cm/yr. Yet, the depth of the basin is 40 m below the surrounding seafloor, suggesting that subsidence is very rapid, faster than its sedimentation rate. Therefore, these small basins have the potential to provide a high-resolution record of seismic activity. Third, as a result of the high sedimentation rates, a chronology can be effectively obtained from the sediments by using short-lived

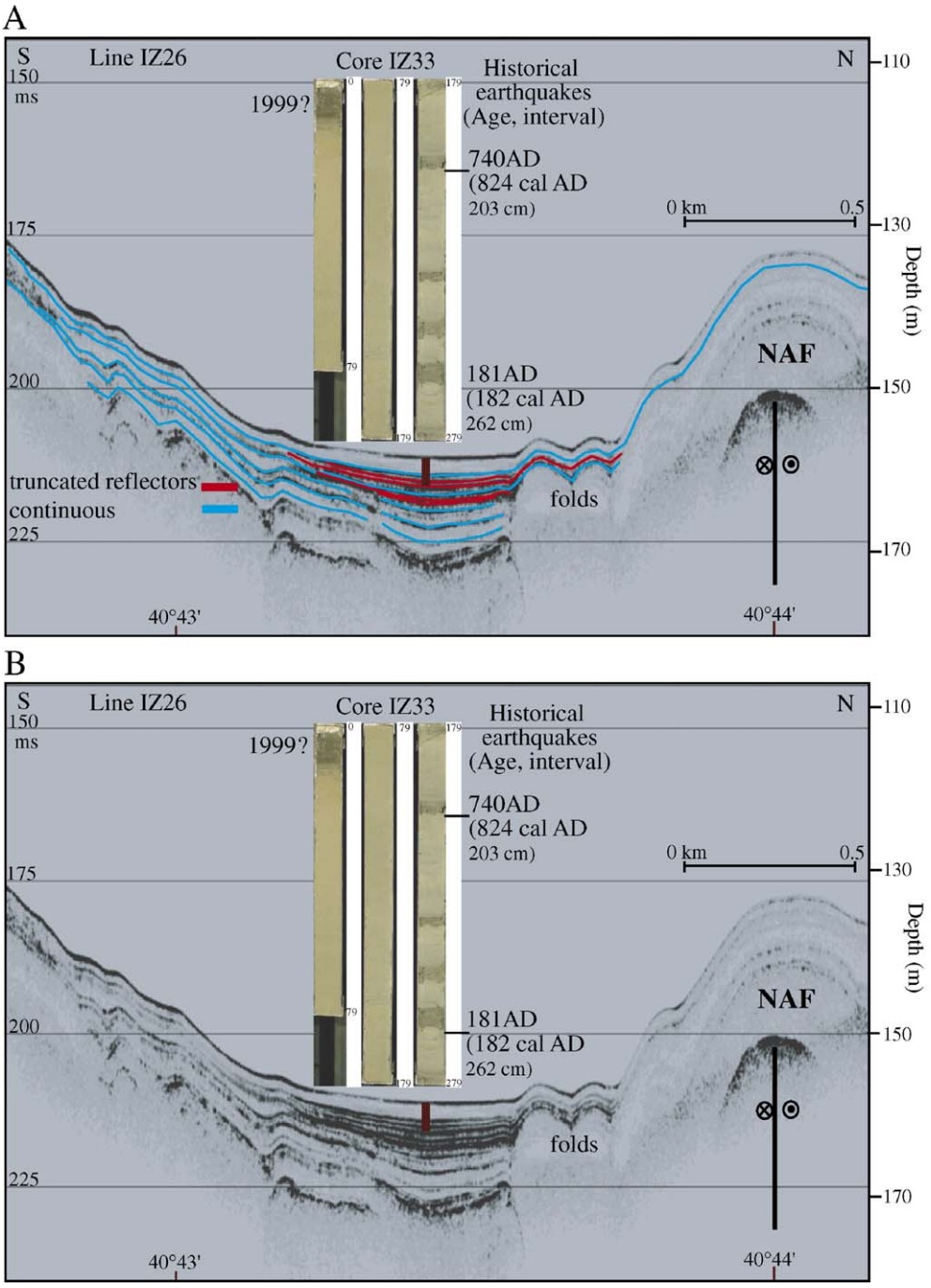

Fig. 10. Subbottom profile Line IZ26 across Izmit Gulf showing seismic reflections that onlap and are tilted towards the fault. Strata is truncated towards the southern margin where slumping occurred. Continuous seismic reflections drape the truncated strata. Correlation to the lithology links the coarser sand beds to earthquake events that led to scour of the basin floor. ^{14}C chronology shows that only surficial sediments are reworked. We linked two of the sand beds to the 181 AD and 740 AD earthquake events. The sand beds are separated by muddy intervals that represent the continuous seismic surfaces that drape the basin. Stratigraphic relations suggest that the event at the top of the core may be the 1999.

radioisotopes and radiocarbon. Fourth, their formation is controlled by the fault rather than downslope processes and therefore the sediments are not as influenced by terrestrial drainage as those of a shelf or slope [87,88]. Holocene deposits from the Ganos Basin lack shore facies sediments such as coarse sands and mollusk shells

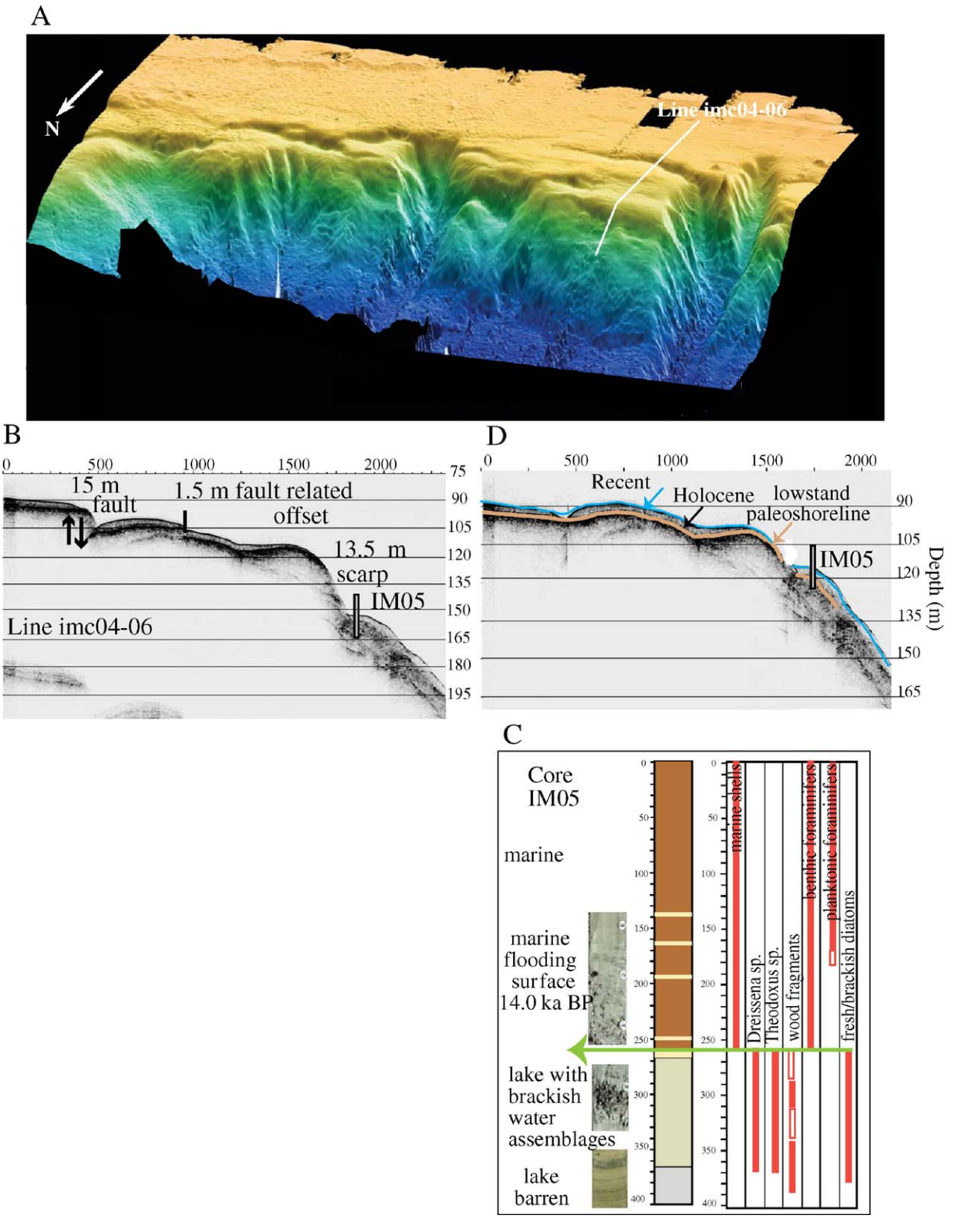
A
N
Line imc04-06
B
0
500
1000
1500
2000
15 m fault
1.5 m fault related offset
13.5 m scarp
IM05
Line imc04-06
75
90
105
120
135
150
165
180
195
D
Recent
Holocene
lowstand paleoshoreline
IM05
Depth (m)
C
Core IM05
marine
marine flooding surface 14.0 ka BP
lake with brackish water assemblages
lake barren
marine shells
Dreissena sp.
Theodoxus sp.
wood fragments
benthic foraminifers
planktonic foraminifers
fresh/brackish diatoms

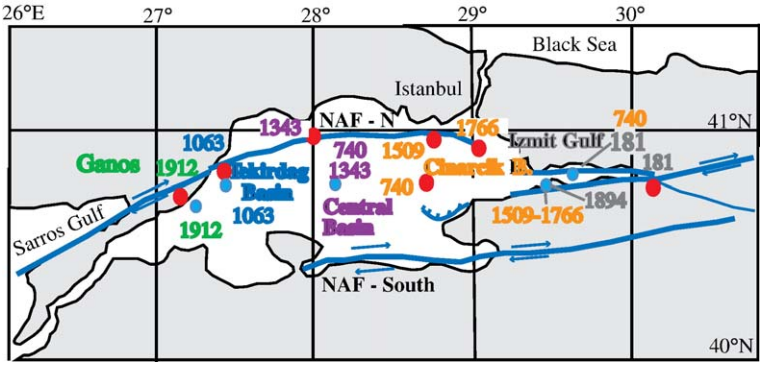

Fig. 12. Map of the Marmara Sea region showing the North Anatolia Fault northern and southern branches. The red dots represent the estimated location of earthquake epicenters based on historical accounts [19–23]. The location of our cores is marked by a blue dot. The events that we were able to correlate to the historical record are colored: Ganos (green), Tekirdag Basin (blue), Central Basin (purple), Cinarcik Basin (orange) and Izmit Gulf (gray). Note the correlation between the areas of maximum damage reported and the location of events we identified. Based on these initial results, we propose that the sedimentary record of large earthquakes is localized to proximal regions to a rupture and that with a high density of cores this record can be used to determine fault segmentation and recurrence interval.

and large pieces of wood material indicating isolation from possible storm derived terrigenous sedimentation events. The 1912 event has been well documented along the Gelibolu Peninsula [21,22,43,44] and the Ganos Basin provides compelling evidence that the rupture extended across the shelf in the western Marmara Sea and supports prior studies that it did extend into Tekirdag Basin [29,43,44].

An unexpected result is that the sampled stratigraphy of the larger Tekirdag and Central Basins did not preserve a record of all earthquakes reported within the Marmara Sea region with estimated magnitudes greater than 7 as was anticipated. More significant for paleoseismology is that the floors of these basins contain the record of those earthquakes with reported areas of maximum damage within the surrounding area (Fig. 12). This suggests that the fill of a transform basin has the potential to document earthquake ruptures along the bounding fault segments. Evidence for this was documented in Tekirdag Basin where a deposit composed of reworked sediment can be linked by radiocarbon dating and grain size variability to a severe earthquake that affected the north coast of the Sea of Marmara in 1063 (Fig. 12). We therefore interpret this stratigraphic event as earthquake-related. The area of maximum damage reported by Ambrassey and Jackson [35] for the 1063 event is to the northwest of Marmara Sea adjacent to Tekirdag Basin. In Central Basin, a homogenite can be linked to the 1343 earthquake event (Fig. 12). The area of maximum damage documented for the 1343 earthquake by Ambraseys and Jackson [19–23] was north of Marmara Sea and west of the Central Basin. Our results coupled to the studies of Ambraseys and Jackson [19–23] suggest that the segment that ruptured in 1343 ruptured the fault branch in the vicinity of Tekirdag and Central Basins. Homogenites from Central Basin and Izmit Gulf are linked to the 740 AD event, which has a documented area of maximum destruction and observed tsunamis to the south of Izmit Gulf and Cinarcik Basin (Fig. 12). This suggests that the 740 AD was a particularly large earthquake that ruptured the NAF through the Gulf of Izmit and the eastern Marmara Sea.

Evidence for recent activity was found west of Hersek Peninsula where sandy mass-flows were correlated to the 1509 event and 1766 earthquake located in the east part of the Marmara Sea (Fig. 12). The 1509 event was particularly destructive and considered a major event with Ms > 7.2. Most importantly, the area of greatest destruction was reported near Istanbul and its

Fig. 11. (A) 3-D perspective view of the Imrali Shelf constructed from multibeam bathymetry and illuminated to the south. The image shows a series of rotational slumps concave towards the basin and the location of Line imc04-06. (B) Line imc04-06 shows footwall collapse along an active normal fault scarp. Profile also shows slumping along a steep slope possibly created by active normal faults. Core IM05 is at the base of the scarp at 150 m of present water depth. (C) Sediment in core IM05 shows no deformation and the lithology, faunal and floral assemblages provide evidence from the base to top of the core: of a barren lake; a lake with brackish water assemblages; a marine flooding surface dated at 14.0 ka BP and noted by a pebbly sand bed. Above, there is an abrupt change to marine fauna and flora (modified after [92,93]). (D) Based on the core data and chirp profiles, we identified the Holocene drape between modern sediments traced in turquoise and the low-stand late Pleistocene paleoshoreline of Marmara Lake traced in brown and dated at 14.0 ka BP. We reconstructed the chirp line for 15 m of vertical fault offset, 1.5 m of fault related displacement and 13.5 m due to sediment sliding. After reconstruction, core IM05 is at −120 m of water depth and the paleoshoreline at −95 m.

epicenter is commonly proposed in Cinarcik Basin [8,21]. The 1766 earthquake, with Ms>7.2, is also inferred to have had an epicentral region west of Istanbul in Cinarcik Basin. The areas of most damage associated to the 1509 and 1766 events were reported at ~40 km from the Hersek Peninsula.

The 181 AD earthquake caused destruction in Nicomedia (Izmit) and the damage extended to the southeast region of Mudurmu [19]. The damage was concentrated to the east and southeast of Izmit Gulf for the 181 AD as well as that of the 1999 earthquakes (Fig. 12). We found concrete evidence for 181 AD and 1894 events in Izmit Gulf (Karamursel Basin and West of Hersek Peninsula) and based on stratigraphic relations possibly the 1999 event (not confirmed by dating). These results indicate that there is a remarkable correlation between the reported historical data and our findings in the Marmara Sea and show that not only large earthquakes are recorded in the sedimentary record but they also can point to the general region of a rupture.

4.2. Sedimentation model for transform basins

The transform basins of Marmara Sea of large, intermediate and small size share distinct characteristics. They are typically asymmetric, their slopes are steep and their floors are gently tilted, except for a relatively small and remarkably horizontal depocentral area that is currently receiving gravity-flow sediment. Seismic profiles and core data indicate that the basin floors generally consist of a stack of characteristic packages that exhibit a small-scale internal stratigraphy similar to the homogenites described by Kastens and Cita for the Mediterranean [80]. We propose that these packages are typical of the basins depocenter and represent the signature of large earthquakes that dominate the sedimentation of transform basins. We outline a model that relates meizoseismal effects with the observed internal stratigraphy of the units, within the context of basin evolution in the Marmara Sea (Fig. 13). A large earthquake moves the sea floor over a wide frequency range, from shaking to permanent changes in morphology. Submarine effects of shaking at high acceleration are not yet well documented, but include: (1) fluidization of unconsolidated sediment as documented in mud volcanoes (e.g., the eruption of mud volcanoes in Makran Coast, as a result of the Pakistan earthquake [96] and in Izmit Gulf [18]); (2) fracturing and mass-wasting of the slope (e.g., extensive fracturing and mass wasting was observed in association to the Sumatra-Andaman earthquake [97]; mass-wasting linked to the 1929 Grand Banks earthquake is very well characterized [98]); (3) high-velocity turbidity currents down these slopes (e.g., 1929 Grand Banks earthquake turbidity current) reached velocities of >60 km/h [99]; (4) scour of canyons and channels along the slope and on the basin floor (e.g., in the Cascadia subduction zone where turbidites eroded the canyons and were linked to specific events [13]); and (5) long-lasting suspension of sediment [100,101]. Sediment fluxes measured in Cariaco Basin after a seismically induced turbidite in 1997 showed high sediment concentrations in the water column for 1 month after the earthquake [100]. Low-frequency motion and vertical deformation of the sea-floor cause tsunamis and seiches [97]. Relatively slow and long-lasting internal seiches are likely in the Marmara Sea, which is characterized by the high-density contrast between saline Mediterranean water and fresher Black Sea water [89–91]. These density contrasts are accentuated by sediment suspended during an earthquake that magnify the effects of internal seiches and by the semi-enclosed morphology of the basins that tend to contain the internal waves.

The sedimentary structures of homogenites, initiated by a sharp basal contact overlaid by multiple sand laminae that fine upwards into a thick wedge of homogenous mud, reveal how earthquakes can be the primary cause leading to the deposition of these unique deposits. After a time measured in minutes to hours, mass-wasting (slides, slumps and debris flows) and high-velocity turbidity currents bearing coarse sediment would reach the basin depocenters along the boundary fault. Although erosion may be extensive along the slope and canyons, it is not pronounced in the basin floors where surficial sediments are entrained and reworked ((Figs. 7 and 8, 10 and 13)). The strong sea-floor shaking resuspends large quantities of sediment including sands and coarse silts derived from the shelves and canyon floors that lead to the deposition of the coarse laminae in the homogenite (Fig. 13A,B). Thus, at the end of the mass-wasting process, much of the sediment comprising the future homogenite should be suspended above the basin floor. Sedimentation will then proceed from the coarsest to the finest suspended sediment. Low dissipation internal seiches may develop during the strong seismic shaking and continue long after the earthquake causing periodic currents near the sea-floor that punctuate the sedimentation process with resuspension events, yielding the layering characteristic of a homogenite (Fig. 13B,C). The fine-grained sediment stirred into suspension by the event could take months after an earthquake to settle forming the thick homogenite deposits that drape the basins. In this model, the basin margins have thin accumulations of

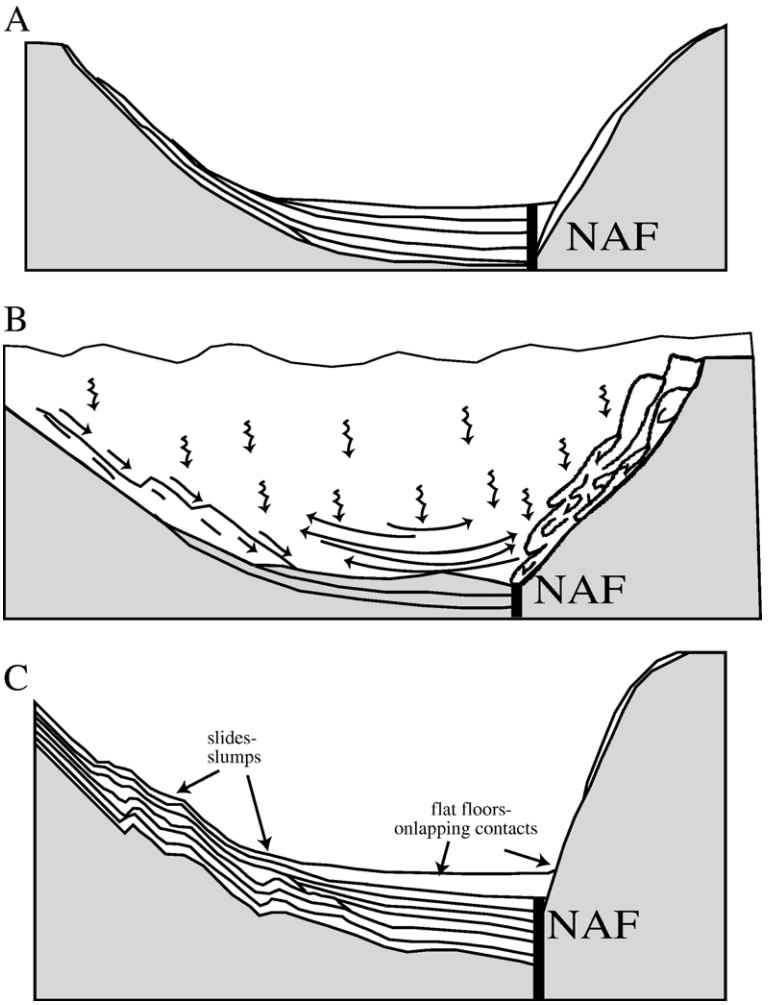

Fig. 13. Sedimentation model for transform basins. (A) Basin depocenters contain a characteristic sequence of multiple sand rich layers that fine upwards into a thick deposit of homogeneous mud. These deposits called "homogenites" are similar to those described by Kastens and Cita [80] for the Mediterranean and represent the signature of large earthquakes that dominate the sedimentation of these basins. (B) An earthquake events trigger failures of the slope (slides, slumps, debris flows) eroding and resuspending sediment. The suspended sediment is gravitationally sorted by seiche currents forming the typical "homogenite" deposit found in the basin floors. The fine-grained material could take months to settle. Pelagic deposition separates the homogenites. Frequent earthquake activity sheds sediments uncovering the slopes and leading to differences in sediment thickness between the margins and depocenters. (C) Typical of semi-enclosed transform basins are the flat floors, onlapping contacts along the boundary fault and steep walls. Rapid, asymmetric subsidence alone could not preserve a flat bottom. Frequent smoothing by seiche currents is thought to be the cause for the flat, smooth basin floors.

sediment due to frequent resuspension by earthquake activity while the basin floors, especially the depocenters, accumulate thick sedimentary deposits. These observations are consistent with sedimentation rates documented by [76,102] and this study that quantified sedimentation rates of 7.5 to 2.5 mm/yr in the basin floors and 0.7 mm/yr on the basin slopes and shoulders. By these processes, submarine earthquakes are thought to cause the upward fining series of sandy and silty layers and lead to the deposition of thick wedges of fine-grained sediments that are characteristic of a homogenite. In the Marmara Sea, only thin (~1 cm) beds of pelagic deposition are preserved in between events. These beds can be identified by clay-sized particles and foraminifers and constitute key horizons for dating earthquake events.

The morphology of the basins' floor typifies semi-enclosed transform basins and earthquake-dominated sedimentation. A gentle slope over much of the basins' floors is generally related to tilting and warping of the basins. In addition, a remarkably horizontal area, the current depocenter of gravity-flow sediment, is clearly

distinguished by high-resolution bathymetry within the basins' floors. These depocenters typically abut the trace of the transform. Sediments form sharp onlapping contacts along the margins of these depocenter areas (Figs. 1, 2, 5, 9 and 10) and do not exhibit sediment aprons and fans extending from submarine canyons and the base of the slope, which characterize most other basins. Rapid, asymmetric subsidence along boundary faults alone could not preserve a flat bottom. The filling of accommodation space created by tilting of the basins by thick homogenite deposits and frequent smoothing by earthquake-triggered seiche currents are thought to be the cause for the horizontal, smooth topography of the sea-floor in these transform basins. The steep-sided walls and asymmetric patterns of the transform basins are primarily controlled by tectonic activity along faults.

The stratigraphic relations indicate that earthquake induced mass-wasting and homogenite deposits may mask evidence of rupture on the basin floor. Thus, subbottom profiling is necessary to detect a rupture and establish its spatial relation with coeval strata related to the same event. Only then, samples can be reliably targeted to date the event. High-resolution geophysical images coupled to precise sampling of sediment are the basic requirements to identify submarine earthquake ruptures.

4.3. Quantification of tectonic activity in transform basins

One of the major goals of this study was to quantify deformation along the submarine portion of the NAF. The integration of geophysics, stratigraphy, and paleoceanography has proven to be an effective method to quantify vertical displacement along the Southern Boundary Fault in Imrali Basin (Fig. 11). A footwall collapse of 15 m measured at the active normal fault scarp indicates a rate of motion of 1 mm/yr in the past 14.0 ka. If the 15 m of vertical offset documented as sliding of blocks is also related to normal fault activity, the rate of vertical displacement can be as high as 2 mm/yr (Fig. 11). The same approach has proven effective in other areas of the Marmara Sea. Offset channels along the NAF in Izmit Gulf were used to measure a minimal dextral strike-slip rate of 10 mm/yr since the Marmara Lake stage [12]. The combination of progressively tilted paleohorizontal surfaces and vertical offset of dated marker horizons, such as the lacustrine paleoshoreline on the shelf and the corresponding gravity-flow sediment horizon near the basins' floor, has quantified oblique-slip kinematics on several segments of the northern branch [18,34]. This pioneering work demonstrates that marine techniques are effective in mapping fault kinematics along a continental transform and is expected to lead to further studies that will fully evaluate vertical and strike-slip deformation of the North Anatolia Fault.

5. Conclusions

An initial effort to understand the sedimentary signature of large earthquakes along segments of the NAF in the Marmara Sea has proven successful: (1) we documented evidence for large historical earthquakes that occurred in 181 AD, 740 AD, 1063 AD, 1343 AD, 1509 AD, 1766 AD, 1894 AD and 1912 AD; (2) the 1912 earthquake rupture was documented in the small transform basin along the Ganos Fault segment of the NAF; (2) the deepest part of the larger Tekirdag and Central transform basins contains a record of strong earthquakes ($Ms > 7$) that occurred along fault segments bounding each basin (1063 AD for Tekirdag Basin, and 740 AD and 1343 AD for Central Basin). This result was unexpected but most promising because it has the potential of documenting which fault segment ruptured when, and the recurrence interval of large events on these fault segments; (3) sedimentation in these transform basins is dominated by earthquake-induced homogenites and seiche-currents that maintain a flat basin floor; (4) the finest grain size (clay) in the Marmara basin-floor sequences is representative of pelagic sedimentation and should be targeted for radiocarbon dating because it has the largest abundance of foraminifers; (5) sedimentation rates are very high, up to 0.5 to 1 cm/yr at the depocenters. Subsidence rates are likely to be even higher and thus to be of comparable magnitude to the horizontal component of slip along the transform. This suggests that the basins are very young; (6) we documented evidence for the 1509 AD, 1766 AD and 1894 AD earthquakes, postulated to have occurred in the vicinity of Cinarcik Basin and the Gulf of Izmit, west of the Hersek Peninsula; and (7) we quantified vertical deformation of 1 mm/yr in the past 14.0 ka along the Southern Boundary Fault by integrating geophysics, stratigraphy and paleoceanography.

This study characterizes ideal sampling sites for submarine earthquake geology. It is critical to target the basin depocenter for maximum thickness of earthquake-related sediments and for avoiding erosional discontinuities. High-resolution geophysics and understanding fault kinematics are prerequisites because the depocenters are generally much smaller than the basin's floor and typically shift along strike in these transform basins. Core profiles are needed to ensure section completeness and to investigate lateral variations in the internal structure

of each erosional-depositional event. Whether a basin preserve the record of all large ruptures in that basin remains to be shown, but preliminary results suggest a close correspondence and that coseismic deformation of the sea-floor may have an important role in generating seismites. Closely spaced transects of precisely positioned, long cores across asymmetric transform basins are needed to investigate lateral variations in the internal structure of each erosional-depositional event and to evaluate the extent to which pelagic sediments are reworked into the seismite. Such '3D sampling' is also necessary to evaluate progressive vertical offset and tilting across a fault.

Acknowledgements

We thank the Turkish Council for Technical and Scientific Research (TÜBITAK) and the General Directorate of Mineral Research and Exploration (MTA) for their assistance and logistic support of this project, as well as the Turkish Department of Navigation, Hydrography and Oceanography (SHOD) for providing their 1999 multibeam bathymetry data. We are grateful to the captains and crews of the *R/V Odin Finder* and of the *R/V Urania* for their efforts in the collection of the data. We gratefully acknowledge the contribution of the scientific parties for both expeditions, which comprised Martina Busetti, Lucilla Capotondi, Kadir Eris, Paola Fabretti, E.J. Fielding, Caner Imren, Hulya Kurt, Marco Ligi, Alessandro Magagnoli, Gabrielle Marozzi, Nilgün Okay, Naside Ozer, Daniella Penitenti, Kerim Sarikavak, Giorgio Serpi and Bugser Tok. We thank the Queens College students that helped in the processing of the data: George Lozefski, Damayanti Gurung, Kalliopi Ziangos and Hsun Chang. Emin Demirbag at Istanbul Technical University kindly provided us with available digital data for the area. NATO Collaborative Linkage Grant #976826 provided seed funding and made this international collaboration possible. Data acquisition and analysis have been jointly financed by US National Science Foundation grants OCE-0096668, OCE-0222285 and OCE-0222139, the Italian National Research Council (CNR), TÜBITAK, Lamont-Doherty Earth Observatory, and City University of New York (PSC-CUNY). This is a Lamont-Doherty Earth Observatory Contribution #6918.

References

[1] J.F. Dolan, K.E. Sieh, T.K. Rockwell, R.S. Yeats, J.H. Shaw, J. Suppe, G. Huftile, E. Gath, Prospects for larger or more frequent earthquakes in greater metropolitan Los Angeles, California, Science 267 (1995) 199–205.

[2] D.J. Wald, H. Kanamori, D.V. Helmberger, Source study of the 1906 San Francisco Earthquake, Bull. Seismol. Soc. Am. 83 (1993) 981–1019.

[3] J. Grases, R. Altez, M. Lugo, Catalogo de Sismos Sentidos o Destructores Venezuela 1530–1988, Academia de Ciencias Fisicas, Matematicas y Naturales; Facultad de Ingenieria; Universidad Central de Venezuela, Caracas, Venezuela, 1999, 654 pp.

[4] C. Mendoza, Rupture history of the 1997 Cariaco, Venezuela, earthquake from teleseismic P waves, Geophys. Res. Lett. 27 (2000) 1555–1558.

[5] D. Hatzfeld, M. Ziiazia, D. Kementzetzidou, P. Hartzidimitrious, D. Papagiotopoulos, K. Makropoulos, P. Papadimitriou, A. Deschamps, Microseismicity and focal mechanisms at the western termination of the North Anatolian Fault and their implications for continental tectonics, Geophys. J. Int. 137 (1999) 891–908.

[6] A.A. Kiratzi, Stress tensor inversions along the northwestern North Anatolian Fault Zone and its continuation into the North Aegean Sea, Geophys. J. Int. 151 (2002) 360–376.

[7] A.A. Barka, K. Kadinsky-Cade, Strike-slip fault geometry in Turkey and its influence on earthquake activity, Tectonics 7 (1988) 663–684.

[8] T. Parsons, S. Toda, R.S. Stein, A.A. Barka, J.H. Dieterich, Heightened odds of large earthquakes near Istanbul: an interaction-based probability calculation, Science 288 (2000) 661–665.

[9] A. Hubert-Ferrari, R. Armijo, G.C.P. King, B. Meyer, A.A. Barka, Morphology, displacement, and slip rates along the North Anatolian Fault, Turkey, J. Geophys. Res. 107 (2002), doi:10.1029/2001JB000393.

[10] B.J. Meade, B.H. Hager, S.C. McClusky, R.E. Reilinger, S. Ergintav, O. Lenk, A.A. Barka, H. Özener, Estimates of seismic potential in the Marmara region from block models of secular deformation constrained by global positioning system measurements, Bull. Seismol. Soc. Am. 92 (2002) 208–215.

[11] T. Parsons, Recalculated probability of $M>7$ earthquakes beneath the Sea of Marmara, Turkey, J. Geophys. Res. 109 (2004), doi:10.1029/2003JB002667.

[12] A. Polonia, L. Gasperini, A. Amorosi, E. Bonatti, G. Bortoluzzi, N. Cagatay, L. Capotondi, M.H. Cormier, N. Gorur, C. McHugh, L. Seeber, Holocene slip rate of the North Anatolian Fault beneath the Sea of Marmara, Earth Planet. Sci. Lett. 227 (2004) 411–426.

[13] C. Goldfinger, C.H. Nelson, J.E. Johnson, The shipboard Scientific Party, Holocene earthquake records from the Cascadia subduction zone and northern San Andreas Fault based on precise dating of offshore turbidites, Annu. Rev. Earth Planet. Sci. 31 (2003) 555–577.

[14] T. Nakajima, Y. Kanai, Sedimentary features of seismoturbidites triggered by the 1983 and older historical earthquakes in the eastern margin of the Japan Sea, Sediment. Geol. 135 (2000) 1–19.

[15] O. Fujiwara, F. Masuda, T. Sakai, T. Irizuki, K. Fuse, Tsunami deposit in Holocene bay mud in southern Kanto region, Pacific coast of central Japan, Sediment. Geol. 135 (2000) 219–230.

[16] D.S. Gorsline, T. De Diego, E.H. Nava-Sanchez, Seismically triggered turbidites in small basins: Alfonso Basin, Western Gulf of California and Santa Monica Basin, California Borderland, Sediment. Geol. 135 (2000) 21–35.

[17] A. Polonia, M.H. Cormier, M.N. Cagatay, G. Bortoluzzi, E. Bonatti, L. Gasperini, L. Seeber, N. Gorur, L. Capotondi, C.M.

G. McHugh, W.B.F. Ryan, O. Emre, N. Okay, M. Ligi, B. Tok, A. Blasi, M. Busetti, K. Eris, P. Fabretti, E.J. Fielding, C. Imren, H. Kurt, A. Magagnoli, G. Marozzi, N. Ozer, D. Penitenti, G. Serpi, K. Sarikavak, Exploring submarine earthquake geology in the Marmara Sea, EOS Trans. AGU 83 (2002) 235–236.

[18] M.-H. Cormier, L. Seeber, C.M.G. McHugh, A. Polonia, M.N. Çagatay, Ö. Emre, L. Gasperini, N. Görür, G. Bortoluzzi, E. Bonatti, W.B.F. Ryan, K.R. Newman, The North Anatolian Fault in the Gulf of Izmit (Turkey): rapid vertical motion in response to minor bends of a non-vertical continental transform, J. Geophys. Res. III (2006) B04102.

[19] N.N. Ambraseys, The seismic activity in the Marmara Sea region over the last 2000 years, Bull. Seismol. Soc. Am. 92 (2002) 1–18.

[20] N.N. Ambraseys, The earthquake of 10 July 1894 in the Gulf of Izmit (Turkey) and its relation to the earthquake of 17 August 1999, J. Seismol. 5 (2001) 117–128.

[21] N.N. Ambraseys, J.A. Jackson, Seismicity of the Sea of Marmara (Turkey) since 1500, Geophys. J. Int. 141 (2000) F1–F6.

[22] N.N. Ambraseys, C.F. Finkel, The Seismicity of Turkey and Adjacent Areas—A Historical Review, 1500–1800, EREN, Istanbul, 1995, 240 pp.

[23] N.N. Ambraseys, C.F. Finkel, Long-term seismicity of Istanbul and the Marmara Sea region, Terra Nova 3 (1991) 527–539.

[24] A.M.C. Sengör, The North Anatolian Transform Fault: its age, offset and tectonic significance, J. Geol. Soc. (Lond.) 136 (1979) 269–282.

[25] A.M.C. Sengör, et al., Strike-slip faulting and related basin formation in zones of tectonic escape: Turkey as a case study, in: K.T. Biddle, N. Christie-Blick (Eds.), Strike-Slip Deformation, Basin Formation, and Sedimentation, The Society of Economic Paleontologists and Mineralogists, 1985, pp. 227–264.

[26] R. Armijo, B. Meyer, A. Hubert, A.A. Barka, Westward propagation of the North Anatolian Fault into the northern Aegean: timing and kinematics, Geology 27 (1999) 267–270.

[27] R. Armijo, B. Meyer, S. Navarro, G.C.P. King, A.A. Barka, Asymmetric slip partitioning in the Sea of Marmara pull-apart: a clue to propagation processes of the North Anatolian Fault? Terra Nova 14 (2002) 80–86.

[28] R. Armijo, F. Flerit, G.C.P. King, B. Meyer, Linear elastic fracture mechanics explains the past and present evolution of the Aegean, Earth Planet. Sci. Lett. 217 (2004) 85–95.

[29] R. Armijo, N. Pondard, B. Meyer, B. Mercier de Lepinay, G. Ucarkus, the MARMARASCARPS Cruise Party, Submarine fault scarps in the Sea of Marmara pull-apart (North Anatolian Fault): implications for seismic hazard in Istanbul, Geochem. Geophys. Geosyst. 6 (2005) 1–29.

[30] X. Le Pichon, A.M.C. Sengör, E. Demirbag, C. Rangin, C. Imren, R. Armijo, N. Görür, M.N. Çagatay, B. Mercier de Lepinay, B. Meyer, R. Saatçilar, B. Tok, The active main Marmara Fault, Earth Planet. Sci. Lett. 192 (2001) 595–616.

[31] X. Le Pichon, N. Chamot-Rooke, C. Rangin, A.M.C. Sengör, The North Anatolian Fault in the Sea of Marmara, J. Geophys. Res. 108 (2003), doi:10.1029/2002JB001862.

[32] C. Yaltirak, Tectonic evolution of the Marmara Sea and its surroundings, Mar. Geol. 190 (2002) 493–529.

[33] D.P. McKenzie, Active tectonics of the Mediterranean region, Geophys. J. R. Astron. Soc. 30 (1972) 109–185.

[34] L. Seeber, Ö. Emre, M.H. Cormier, C.C. Sorlien, C.M.G. McHugh, A. Polonia, N. Özer, M.N. Çagatay, The team of the 2000 R/V Urania cruise in the Marmara Sea, uplift and subsidence from oblique slip: the Ganos-Marmara Bend of the North Anatolian Transform, western Turkey, Tectonophysics 391 (2004) 239–258.

[35] R.E. Reilinger, S.C. McClusky, M.B. Oral, R.W. King, M.N. Toksöz, A.A. Barka, I. Kinik, O. Lenk, I. Sanli, Global positioning system measurements of present-day crustal movements in the Arabia–Africa–Eurasia plate collision zone, J. Geophys. Res. 102 (1997) 9983–9999.

[36] C. Straub, H.G. Kahle, C. Schindler, GPS and geologic estimates of the tectonic activity in the Marmara Sea region, NW Anatolia, J. Geophys. Res. 102 (B12) (1997) 27587–27601.

[37] S.C. McClusky, S. Bassalanian, A.A. Barka, C. Demir, S. Ergintav, I. Georgiev, O. Gurkan, M. Hamburger, K. Hurst, H. G. Kahle, K. Kastens, G. Kekelidze, R.W. King, V. Kotzev, O. Lenk, S. Mahmoud, A. Mishin, M. Nadariya, A. Ouzounis, D. Paradissis, Y. Peter, M. Prilepin, R.E. Reilinger, I. Sanli, H. Seeger, A. Tealeb, M.N. Toksöz, G. Veis, Global positioning system constraints on plate kinematics and dynamics in the eastern Mediterranean and Caucasus, J. Geophys. Res. 105 (2000) 5695–5719.

[38] A.S. Provost, J. Chéry, R. Hassani, 3D mechanical modeling of the GPS velocity field along the North Anatolian Fault, Earth Planet. Sci. Lett. 209 (2003) 361–377.

[39] F. Flerit, R. Armijo, G.C.P. King, B. Meyer, The mechanical interaction between the propagating North Anatolian Fault and the back-arc extension in the Aegean, Earth Planet. Sci. Lett. 224 (2004) 347–362.

[40] A.A. Barka, The 17 August 1999 Izmit earthquake, Science 285 (1999) 1858–1859.

[41] M.N. Toksöz, R.E. Reilinger, C.G. Doll, A.A. Barka, N. Yalcin, Izmit (Turkey) earthquake of 17 August 1999: first report, Seismol. Res. Lett. 70 (1999) 669–679.

[42] R.E. Reilinger, M.N. Toksöz, S.C. McClusky, A.A. Barka, 1999 Izmit, Turkey earthquake was no surprise, GSA Today 10 (2000) 1–6.

[43] T.K. Rockwell, A.A. Barka, A.G. Dawson, H.S. Akyüz, K. Thorup, Paleoseismology of the Gazikoy-Saros segment of the North Anatolian Fault, northwest Turkey: comparison of the historical and paleoseismic records, implications of regional seismic hazard, and models of earthquake recurrence, J. Seismol. 5 (2001) 433–448.

[44] E. Altunel, M. Meghraoui, H.S. Akyüz, A. Dikbas, Characteristics of the 1912 co-seismic rupture along the North Anatolian Fault Zone (Turkey): implications for the expected Marmara earthquake, Terra Nova 16 (2004) 198–204.

[45] A. Hubert-Ferrari, A.A. Barka, E. Jacques, S.S. Nalbant, B. Meyer, R. Armijo, P. Tapponier, G.C.P. King, Seismic hazard in the Marmara Sea region following the 17 August 1999 Izmit earthquake, Nature 404 (2000) 269–273.

[46] K.E. Sieh, A review of geological evidence for recurrence times for large earthquakes, in: D.W. Simpson, P.G. Richards (Eds.), Earthquake Prediction, An International Review, Maurice Ewing Series, vol. 4, American Geophysical Union, Washington, DC, 1981, pp. 181–207.

[47] K. Sieh, The repetition of large-earthquake ruptures, Proc. Natl. Acad. Sci. 93 (1996) 3764–3771.

[48] J.P. McCalpin, Paleoseismology, Academic Press, 1996, 588 pp.

[49] R.S. Yeats, C.R. Allen, K.E. Sieh, Earthquake Geology, Oxford University Press, New York, 1997, 568 pp.

[50] K. Sieh, What happened and what's next? Nature 434 (2005) 573–574.
[51] E. Chapron, C. Beck, M. Pouchet, J.F. Deconninck, 1822 earthquake-triggered homogenite in Lake Le Bouget (NW Alps), Terra Nova 11 (1999) 86–92.
[52] F. Arnaud, V. Lignier, M. Revel, M. Desmet, C. Beck, M. Purchet, F. Charlet, A. Trentesaux, N. Tribovillard, Flood and earthquake disturbance of ^{210}Pb geochronology (Lake Anterne, NW Alps), Terra Nova 14 (2002) 225–232.
[53] J. Goff, C. Chague-Goff, S. Nichol, Paleotsunami deposits: a New Zealand perspective, Sediment. Geol. 143 (2001) 1–6.
[54] W. Heike, F. Werner, The Augias megaturbidite in the Central Ionian Sea (central Mediterranean) and its relation to the Holocene Santorini event, Sediment. Geol. 135 (2000) 205–218.
[55] S. Leroy, N. Kazanci, O. Ileri, M. Kibar, O. Emre, E. McGee, H. I. Griffiths, Abrupt environmental changes within a late Holocene lacustrine sequence south of the Marmara Sea (Lake Manyas, N-W Turkey): possible links with seismic events, Mar. Geol. 190 (2002) 531–552.
[56] S. Marco, M. Stein, A. Agnon, H. Ron, Long-term earthquake clustering: a 50,000-year paleoseismic record in the Dead Sea graben, J. Geophys. Res. 101 (1996) 6179–6191.
[57] S. Marco, T.K. Rockwell, A. Heimann, U. Frieslander, A. Agnon, Late Holocene activity of the Dead Sea Transform revealed in 3D paleoseismic trenches on the Jordan Gorge segment, Earth Planet. Sci. Lett. 234 (2005) 189–205.
[58] R. Ken-Tor, A. Agnon, Y. Enzel, M. Stein, High-resolution geological record of historic earthquakes in the Dead Sea Basin, J. Geophys. Res. 106 (2001) 2221–2234.
[59] C. Migowski, A. Agnon, R. Bookman, J.F.W. Negendank, M. Stein, Recurrence pattern of Holocene earthquakes along the Dead Sea transform revealed by varve-counting and radiocarbon dating of lacustrine sediments, Earth Planet. Sci. Lett. 222 (2004) 301–314.
[60] E. Bard, Geochemical and geophysical implications of the radiocarbon calibration, Geochim. Cosmochim. Acta 62 (1998) 2025–2038.
[61] G. Siani, M. Paterne, M. Arnold, E. Bard, B. Metivier, N. Tisnerat, F. Bassinot, Radiocarbon reservoir ages in the Mediterranean Sea and Black Sea, Radiocarbon 42 (2000) 271–280.
[62] H. Oeschger, U. Siegenthaler, U. Schotterer, A. Guglemann, A box-diffusion model to study the carbon dioxide exchange in nature, Tellus 27 (1975) 168–192.
[63] M. Stuvier, G.W. Pearson, T.F. Braziunas, Radiocarbon age calibration of marine samples back to 9000 cal yr BP, in: M. Stuvier, R.S. Kra (Eds.), Radiocarbon, vol. 28, 1986, pp. 980–1021.
[64] M. Stuvier, P.J. Reimer, R. Reimer, CALIB Radiocarbon Calibration 5.0.2, http://radiocarbon.pa.qub.ac.uk (2005).
[65] K.O. Buesseler, H.D. Livingston, S. Honjo, B.J. Hay, S.J. Manganini, E. Degens, V. Ittekkot, E. Izdar, T. Konuk, Chernobyl radionuclides in a Black Sea sediment trap, Nature 329 (1987) 825–828.
[66] V.N. Eremeev, L.M. Ivanov, A.D. Kirwan, T.M. Margolina, Amount of ^{137}Cs and ^{134}Cs radionuclides in the Black Sea produced by the Chernobyl accident, J. Environ. Radioact. 27 (1995) 49–63.
[67] E.V. Stanev, K.O. Buesseler, J.V. Staneva, H.D. Livingston, The application of radiotracers to a study of Black Sea circulation: validation of numerical simulations against observed weapons testing and Chernobyl ^{137}Cs data, J. Geophys. Res. 104 (1995) C5.
[68] J.F. Crusius, Evaluating the mobility of ^{137}Cs, $^{239+240}$Pu and ^{210}Pb from their distributions in laminated sediments. Ph.D. Dissertation, Columbia University, 1992, p. 261.
[69] P.G. Appleby, Radiometric dating of sediment records in European mountain lakes, in: A. Lami, N. Cameron, A. Korhola (Eds.), Paleolimnology and Ecosystem Dynamics at Remote European Alpine Lakes, Limnology, vol. 59, 2000, pp. 1–14.
[70] F. Arnaud, V. Lignier, M. Revel, M. Desmet, C. Beck, M. Pourchet, F. Charlet, A. Trentesaux, N. Tribovillard, Flood and earthquake disturbance of ^{210}Pb geochronology (Lake Anterne, NW Alps), Terra Nova 14 (2002) 225–232.
[71] S. Marco, A. Agnon, Prehistoric earthquake deformations near Masada, Dead Sea graben, Geology 23 (1995) 695–698.
[72] S.F. Greb, Developing a classification scheme for seismites, GSA Joint Annual Meeting. Paper No. 42-0, 2002.
[73] H.K. Wong, T. Lüdmann, A. Ulug, N. Görür, The Sea of Marmara: a plate boundary sea in an escape tectonic regime, Tectonophysics 244 (1995) 231–250, doi:10.1016/0040-1951(94)00245-5.
[74] A.I. Okay, E. Demirbag, H. Kurt, N. Okay, I. Kusçu, An active, deep marine strike-slip basin along the North Anatolian Fault in Turkey, Tectonics 18 (1999) 129–147.
[75] A.I. Okay, A. Kaslilar-Özcan, C. Imren, A. Boztepe-Güney, E. Demirbag, I. Kusçu, Active faults and evolving strike-slip basins in the Marmara Sea, northwest Turkey: a multichannel seismic reflection study, Tectonophysics 321 (2000) 189–218.
[76] M.N. Cagatay, N. Görür, O. Algan, C.J. Eastoe, A. Tchapalyga, D. Ongan, T. Kuhn, I. Kusçu, Late Glacial–Holocene paleoceanography of the Sea of Marmara: timing of connections with the Mediterranean and the Black Seas, Mar. Geol. 167 (2002) 191–206.
[77] M.N. Cagatay, N. Görür, A. Polonia, E. Demirbag, M. Sakinç, M.H. Cormier, L. Capotondi, C.M.G. McHugh, Ö. Emre, K. Eris, Sea-level changes and depositional environments in the Izmit Gulf, eastern Marmara Sea, during the late glacial–Holocene period, Mar. Geol. 202 (2003) 159–173.
[78] E. Gökasan, B. Alpar, C. Gazioglu, Z.Y. Yücel, B. Tok, E. Dogan, A.C. Güneysu, Active tectonics of the Izmit Gulf (NE Marmara Sea): from high resolution seismic and multi-beam bathymetry data, Mar. Geol. 175 (2001) 273–296.
[79] I. Kusçu, M. Okamura, H. Matsuoka, Y. Awata, Active faults in the Gulf of Izmit on the North Anatolian Fault, NW Turkey: a high-resolution shallow seismic study, Mar. Geol. 190 (1–2) (2002) 421–443.
[80] K.A. Kastens, M.B. Cita, Tsunami-induced sediment transport in the abyssal Mediterranean Sea, Bull. Geol. Soc. Am. 92 (1981) 845–857.
[81] M.B. Cita, A. Camerlenghi, B. Rimoldi, Deep-sea tsunami deposits in the eastern Mediterranean: new evidence and depositional models, Sediment. Geol. 104 (1996) 155–173.
[82] M.B. Cita, B. Rimoldi, Geological and geophysical evidence for a Holocene tsunami deposit in the eastern Mediterranean and deep-sea record, J. Geodyn. 24 (1997) 293–304.
[83] C. Beck, J.L. Schneider, B. Mercier de Lepinay, N. Cagatay, L. Labeyrie, J.L. Turon, E. Wendenbaum, S. Boutareau, G. Menot-Combes, I. Hadjas, MARMARCORE Scientific Party, Geophys. Res. Abstr. 5 (2003) 12778.
[84] S. Marco, A. Agnon, Prehistoric earthquake deformations near Masada, Dead Sea graben, Geology 23 (1995) 695–698.

[85] S.F. Greb, Developing a classification scheme for seismites, GSA Joint Annual Meeting, Paper No. 42, 2002.
[86] A.I. Okay, O. Tüysüz, S. Kaya, From transpression to transtension: changes in morphology and structure around a bend on the North Anatolian Fault in the Marmara region, Tectonophysics 391 (2004) 259–282.
[87] J. Dutton, C. McHugh, M.-H. Cormier, L. Seeber, N. Cagatay, N. Okay, K. Ziangos, Developing tools for paleoseismology in the submarine environment, case studies: North Anatolian Fault Zone, Marmara Sea, Turkey and El Pilar Fault, Cariaco Basin, Venezuela, Abstr. Programs-Geol. Soc. Am. 36 (2004) (Abstract No. 70072).
[88] J. Dutton, Developing tools for paleoseismology in the submarine environment, case studies: North Anatolian Fault Zone, Marmara Sea, Turkey and El Pilar Fault, Cariaco Basin, Venezuela, M.A. Thesis, Queens College, CUNY, 2006, 75 pp.
[89] M.N. Cagatay, O. Algan, M. Sakinç, C.J. Eastoe, L. Egesel, N. Balkis, D. Ongan, H. Caner, A mid–late Holocene sapropelic sediment unit from the southern Marmara sea shelf and its paleoceanographic significance, Quat. Sci. Rev. 18 (1999) 531–540.
[90] W.B.F. Ryan, W.C. Pitman, C.O. Major, K. Shimkus, V. Moskalenko, G.A. Jones, P. Dimitrov, N. Gorur, M. Sakinc, H. Yuce, An abrupt drowning of the Black Sea Shelf, Mar. Geol. 138 (1997) 119–126.
[91] A.E. Aksu, R.N. Hiscott, D. Yasar, Oscillating Quaternary water levels of the Marmara Sea and vigorous outflow into the Aegean Sea from the Marmara–Black Sea drainage corridor, Mar. Geol. 153 (1999) 275–302.
[92] C.M.G. McHugh, D. Gurung, W.B.F. Ryan, U. Sancar, L. Burckle, M.N. Cagatay, L. Capotondi, R.V. Urania, MARMARA 2001 Team, Late Pleistocene to Holocene lacustrine to marine transition in the Marmara Sea: implications for climate and water mass exchange, Geophys. Res. Abstr. 6 (2004) 05897.
[93] C.M. McHugh, Y. Mart, W.B. Ryan, L. Giosan, D. Gurung, M. N. Cagatay, D. Vachtman, U. Sancar, K. Eris, L. Burckle, L. Capotondi, Reconnections of marginal basins to the world ocean: new data from the Marmara Sea, EOS Trans. AGU 86 (52) (2005) 33A–1548.
[94] D.A. Ross, E.T.D.A. Degens, Recent sediments of the Black Sea, in: E.T. Degens, D.A. Ross (Eds.), The Black Sea Geology, Chemistry and Biology, Tulsa, Mem.-Am. Assoc. Pet. Geol., 1974, pp. 183–199.
[95] P.V. Federov, Postglacial transgression of the Black Sea, Int. Geol. Rev. 14 (1971) 160–164.
[96] R.C. Quittmeyer, K.H. Jacob, Historical and modern seismicity of Pakistan, Afghanistan, northwestern India, and southeastern Iran, Bull. Seismol. Soc. Am. 69 (1979) 773–823.
[97] K. Sieh, What happened and what's next? Nature 434 (2005) 573–574.
[98] D.J.W. Piper, P. Cochonat, M.L. Morrison, The sequence of events around the epicenter of the 1929 Grand Banks earthquake: initiation of debris flows and turbidity current inferred from side-scan sonar, Sedimentology 46 (1999) 79–97.
[99] B. Heezen, M. Ewing, Turbidity currents and submarine slumps, and the 1929 Grand Banks earthquake, Am. J. Sci. 250 (1952) 849–873.
[100] R. Thunell, E. Tappa, R. Varela, M. Llano, Y. Astor, F. Muller-Karger, R. Bohrer, Increased marine sediment suspension and fluxes following an earthquake, Nature 398 (1999) 233–236.
[101] M. Itou, I. Matsumura, S. Noriki, A large flux of particulate matter in the deep Japan Trench observed just after the 1994 Sanriku-Oki earthquake, Deep-Sea Res. I 47 (2000) 1987–1998.
[102] B. Mercier de Lepinay, L. Labeyrie, N. Cagatay, MARMACORE Team, Interplay between recent sedimentation and active tectonics in Marmara Sea, Geophys. Res. Abstr. 5 (2003) 13126.